

UNIVERSIDADE FEDERAL DO RIO GRANDE DO SUL  
FACULDADE DE ODONTOLOGIA  
LABORATÓRIO DE MATERIAIS DENTÁRIOS

VICTÓRIA BRITZ RÜCKER

CIMENTO ENDODÔNTICO RESINOSO EXPERIMENTAL CONTENDO  
NANOPARTÍCULAS CORE-SHELL DE PRATA

Porto Alegre

2022

VICTÓRIA BRITZ RÜCKER

CIMENTO ENDODÔNTICO RESINOSO EXPERIMENTAL CONTENDO  
NANOPARTÍCULAS CORE-SHELL DE PRATA

Trabalho de Conclusão de Curso apresentado ao Curso de Odontologia da Universidade Federal do Rio Grande do Sul, como requisito parcial para obtenção do título de Cirurgiã-Dentista.

Orientador: Vicente Castelo Branco Leitune

Porto Alegre

2022

### CIP - Catalogação na Publicação

Britz Rücker, Victória  
CIMENTO ENDODÔNTICO RESINOSO EXPERIMENTAL CONTENDO  
NANOPARTÍCULAS CORE-SHELL DE PRATA / Victória Britz  
Rücker. -- 2022.  
51 f.  
Orientador: Vicente Castelo Branco Leitune.

Trabalho de conclusão de curso (Graduação) --  
Universidade Federal do Rio Grande do Sul, Faculdade  
de Odontologia, Curso de Odontologia, Porto Alegre,  
BR-RS, 2022.

1. Materiais Dentários. 2. Cimento endodôntico. 3.  
Prata. 4. Nanopartículas core-shell. 5.  
Antibacterianos. I. Castelo Branco Leitune, Vicente,  
orient. II. Título.

VICTÓRIA BRITZ RÜCKER

CIMENTO ENDODÔNTICO RESINOSO EXPERIMENTAL CONTENDO  
NANOPARTÍCULAS CORE-SHELL DE PRATA

Trabalho de Conclusão de Curso apresentado ao Curso de Odontologia da Universidade Federal do Rio Grande do Sul, como requisito parcial para obtenção do título de Cirurgiã-Dentista.

Porto Alegre, 05 de outubro de 2022.

---

Vicente Castelo Branco Leitune

Doutor em Odontologia. Universidade Federal do Rio Grande do Sul.

---

Francisco Montagner

Doutor em Odontologia. Universidade Federal do Rio Grande do Sul.

---

Gabriela de Souza Balbinot

Doutora em Odontologia. Universidade Federal do Rio Grande do Sul.

A quem me espelho diariamente, minha mãe.

## **AGRADECIMENTOS**

Agradeço a todos que torceram por esta conquista e que, de alguma forma, se fizeram presentes e me ajudaram nesta caminhada.

Aos meus professores Vicente, Gabriela e Fabrício por me incentivarem a sempre dar o meu melhor, e aos colegas do Laboratório de Materiais Dentários, por compartilharem dessa trajetória comigo.

Ao meu namorado Lucas, por me tranquilizar em todos os momentos e por nunca duvidar do meu potencial.

Às minhas amigas e amigos, por tornarem a vida mais divertida e por estarem comigo nos bons e maus tempos.

Ao meu pai, por todo o carinho que me deu e que ainda sinto, mesmo tão distante. Espero que comemore esta vitória que também é tua, de onde quer que esteja.

E principalmente à minha mãe, a mulher da minha vida e meu maior exemplo de força e amor. A pessoa que nunca mediu esforços para me ver feliz, que me permitiu ser livre para escolher os meus caminhos e que me apoiou em todos os meus passos até aqui.

“Para enxergar claro, basta mudar a direção do olhar.”

Antoine de Saint-Exupéry

## RESUMO

O objetivo do estudo foi sintetizar e caracterizar nanopartículas *core-shell* de prata ( $\text{Ag@SiO}_2$ ) e adicioná-las em um cimento endodôntico experimental. As  $\text{Ag@SiO}_2$  foram produzidas por meio do processo de sol-gel e caracterizadas quanto à sua estrutura química por espectroscopia de infravermelho por transformada de Fourier (FTIR), difração de raios X (DRX), microscopia eletrônica de varredura (MEV), microscopia eletrônica de transmissão (MET), análise termogravimétrica (TGA), termogravimetria derivada (DTG) e espectroscopia UV/visível. Formulou-se um cimento resinoso endodôntico experimental de cura dual, utilizando 70% de UDMA, 15% de GDMA e 15% de BisEMA. As  $\text{Ag@SiO}_2$  foram incorporadas ao cimento endodôntico nas concentrações 2,5%, 5% e 10% em peso. Um grupo foi formulado sem adição de  $\text{Ag@SiO}_2$  (grupo 0%). Os grupos foram avaliados quanto ao escoamento, espessura de película, grau de conversão, amolecimento em solvente, radiopacidade, citotoxicidade para fibroblastos e atividade antibacteriana contra *E. faecalis*. Através do FTIR visualizamos, na análise das  $\text{Ag@SiO}_2$ , o pico referente a ligação Si-O-Si deslocado, indicando a presença de prata no interior das nanopartículas de sílica. Na análise de DRX foi encontrada uma estrutura amorfa para nanopartículas de sílica pura e uma estrutura cristalina apresentando uma estrutura cúbica de face centrada para as  $\text{Ag@SiO}_2$ . Nas análises de TGA e DTG, após a temperatura atingir 200 °C, nanopartículas de sílica pura apresentaram perda de massa característica, já as  $\text{Ag@SiO}_2$  apresentaram perda de massa exacerbada, sendo atribuída à perda da estrutura *core-shell*. Nas imagens de MEV e MET podemos observar partículas esféricas e organizadas, com uma casca cinza e uma estrutura central mais escura. O diâmetro médio das partículas sintetizadas encontrado foi de  $683,51 \pm 93,58$  nm. Quanto ao teste de espectroscopia UV/visível, na análise das  $\text{Ag@SiO}_2$ , observou-se o pico principal em 405 nm, comprimento de onda característico da prata. O escoamento e a espessura de película de todos os grupos do cimento apresentaram resultados dentro do estabelecido pela ISO 6876, porém a radiopacidade não atingiu os valores de referência. Houve diminuição na microdureza Knoop após imersão no solvente ( $p < 0,05$ ) em todos os grupos. O grupo de 10% apresentou um resultado maior para  $\Delta\text{KHN}\%$ . O grau de conversão variou de  $40,82\% \pm 17,84$  a  $63,92\% \pm 9,94$  nos grupos testados, sendo estes valores semelhantes aos encontrados para cimentos comerciais e não havendo diferença estatisticamente significativa entre eles. Não foi observada redução da viabilidade celular nos grupos testados ( $p > 0,05$ ). Observamos aumento na ação antibacteriana com a adição de  $\text{Ag@SiO}_2$  em 10% na análise imediata (24h) e após 9 meses ( $p < 0,05$ ). As nanopartículas *core-shell* de prata foram sintetizadas adequadamente e a incorporação de 10%



em peso reduziu a viabilidade de *E. faecalis* tanto na análise imediata quanto longitudinal, mantendo as propriedades físico-químicas dos cimentos desenvolvidos.

**Palavras-chave:** Materiais Dentários; Prata; Nanopartículas; Antibacterianos; *Enterococcus faecalis*.

## ABSTRACT

The aim of the study was to synthesize and characterize silver *core-shell* nanoparticles (Ag@SiO<sub>2</sub>) and incorporate them into an experimental endodontic sealer. The Ag@SiO<sub>2</sub> were produced through the sol-gel process and characterized in terms of their chemical structure by Fourier transform infrared spectroscopy (FTIR), X-ray diffraction (XRD), scanning electron microscopy (SEM), transmission electron microscopy (TEM), thermogravimetric analysis (TGA), derivative thermogravimetry (DTG), and UV/visible spectroscopy. An experimental dual-cure resin endodontic sealer was formulated using 70% UDMA, 15% GDMA, and 15% BisEMA. Ag@SiO<sub>2</sub> were incorporated into the endodontic sealer at concentrations of 2.5%, 5%, and 10% by weight. One group was formulated without the addition of Ag@SiO<sub>2</sub> (0% group). The groups were evaluated for their flow, film thickness, degree of conversion, softening in solvent, radiopacity, cytotoxicity for fibroblasts, and antibacterial activity against *E. faecalis*. Through the FTIR we visualized, in the analysis of Ag@SiO<sub>2</sub>, a shift on the peak referring to the Si-O-Si bond, indicating the presence of silver inside the silica nanoparticles. In the XRD analysis, an amorphous structure was found for pure silica nanoparticles and a crystalline structure with the presence of a face-centered cubic structure for Ag@SiO<sub>2</sub>. In the TGA and DTG analysis, after the temperature reaches 200 °C, pure silica nanoparticles showed a characteristic loss of mass, while the Ag@SiO<sub>2</sub> showed an exacerbated loss, being assigned to the loss of *core-shell* structure. In the SEM and TEM images, we can observe spherical and organized particles, with a gray shell and a darker core structure. The average diameter of the synthesized particles found was  $683.51 \pm 93.58$  nm. As for the UV/visible spectroscopy test, in the analysis of Ag@SiO<sub>2</sub>, the main peak was observed at 405 nm, a characteristic wavelength of silver. The flow and film thickness of all the groups showed results within the recommended by ISO 6876, but the radiopacity values were below the ones required values by the norm. There was a decrease in Knoop microhardness after immersion in solvent ( $p < 0.05$ ) in all groups. The 10% group presented a higher result for  $\Delta KHN\%$ . The degree of conversion ranged from  $40.82\% \pm 17.84$  to  $63.92\% \pm 9.94$  in the groups tested, with values similar to those found for commercial sealers and with no statistically significant difference between them. No reduction in cell viability was observed in the groups tested ( $p > 0.05$ ). We observed an increase in antibacterial activity with the addition of 10 wt% Ag@SiO<sub>2</sub> in the immediate (24 h) and longitudinal (9 months) analysis ( $p < 0.05$ ). The silver *core-shell* nanoparticles were synthesized adequately and the incorporation of 10 wt% reduced *E. faecalis* viability at

immediate and longitudinal analysis, maintaining the physicochemical properties for developed sealers.

**Keywords:** Dental Materials; Silver; Nanoparticles; Antibacterial Agents; *Enterococcus faecalis*.

## SUMÁRIO

<b>1. INTRODUÇÃO .....</b>	<b>12</b>
<b>2. OBJETIVO .....</b>	<b>14</b>
<b>3. ARTIGO CIENTÍFICO.....</b>	<b>14</b>
<b>4. CONSIDERAÇÕES FINAIS.....</b>	<b>46</b>
<b>REFERÊNCIAS .....</b>	<b>47</b>

## 1 INTRODUÇÃO

O tratamento endodôntico apresenta altas taxas de sucesso, em torno de 86% (ELEMAM; PRETTY, 2011), porém alguns fatores podem causar a sua falha (SIQUEIRA, 2001), ocasionando uma reinfecção e exigindo uma nova intervenção. Quando ocorre o insucesso do tratamento endodôntico, os fatores usualmente associados são: persistência de bactérias (intra-canal e extra-canal), obturação inadequada do canal, excesso de material obturador, selamento coronário inadequado, presença de canais não tratados (principais ou acessórios), iatrogenia durante o procedimento e intercorrências durante a instrumentação (TABASSUM; KHAN, 2016). A persistência de bactérias e microrganismos no sistema de canais radiculares após o tratamento é a principal causa destas falhas (SIQUEIRA, 2001), principalmente quando estes microrganismos se apresentam na forma de biofilmes (RICUCCI et al., 2009). Bactérias residuais podem ser encontradas mesmo após um tratamento endodôntico realizado corretamente. Isso ocorre devido à complexidade do sistema de canais radiculares, que podem possuir além dos canais principais, canais acessórios e ramificações (NAIR, 2006).

Sabe-se que a microbiota presente nos canais radiculares infectados e também nas reinfecções é composta principalmente por bactérias anaeróbias, sendo o *Enterococcus faecalis* uma das mais prevalentes (ABDULWAHAB et al., 2021; SUNDQVIST et al., 1998). O *Enterococcus faecalis* apresenta alta capacidade de causar reinfecção mesmo quando os canais radiculares são preparados e obturados adequadamente. Além disso, essa bactéria tem a habilidade de penetrar nos túbulos dentinários (RODRIGUES et al., 2018; SEDGLEY; LENNAN; APPELBE, 2005) e de produzir biofilmes (ABDULLAH et al., 2005; DE PAZ, 2007; WILSON et al., 2015), tornando a infecção mais difícil de ser combatida pois sabe-se que bactérias associadas a biofilmes são mais resistentes (ABDULLAH et al., 2005).

Diversos agentes antibacterianos vêm sendo incorporados aos materiais dentários e, para melhorar os mecanismos de ação destes agentes, sistemas inovadores foram desenvolvidos, como as nanopartículas. Os nanomateriais são definidos como partículas com dimensões de 1 a 1000 nm, apresentando assim tamanhos pequenos, com uma maior relação entre área e volume e potencial bactericida aumentado (ABBASI et al., 2014; ANTON; BENOIT; SAULNIER, 2008; JEEVANANDAM et al., 2018; KIM et al., 2007; RAI et al., 2012; SHRESTHA; KISHEN, 2016).

O uso da prata como agente antibacteriano é bastante difundido na área médica e odontológica (COHEN et al., 2007; KLASSEN, 2000; KRIS N. J. STEVENS et al., 2009;

SILVER; PHUNG; SILVER, 2006). As nanopartículas de prata de tamanho entre 10-100 nm têm forte potencial bactericida contra bactérias gram-positivas e gram-negativas (MONTEIRO et al., 2009; RAI et al., 2012). A atividade destas nanopartículas contra o *Enterococcus faecalis* também já foi testada (BARAS et al., 2019; CORRÊA et al., 2015; LOYOLA-RODRÍGUEZ et al., 2019; SHRESTHA; KISHEN, 2016). A prata possui a capacidade de penetrar na parede celular bacteriana e interage com a membrana celular causando alterações estruturais (JUNG et al., 2008; LU et al., 2013; RAI et al., 2012). As nanopartículas também interagem com o DNA bacteriano, impedindo sua replicação (MORONES et al., 2005; SHRIVASTAVA et al., 2007) e evitando a síntese proteica (SHRIVASTAVA et al., 2007; YAMANAKA; HARA; KUDO, 2005).

Embora as nanopartículas de prata possuam ação antibacteriana comprovada e se apresentem como uma boa estratégia para o uso em materiais antibacterianos, estas podem apresentar efeitos citotóxicos para as células humanas presentes nos tecidos periapicais (ALLAKER, 2010; KIRMANIDOU et al., 2019). O fato de as nanopartículas apresentarem maior área de superfície resulta em maior grau de interação com as células (KIM et al., 2007; TAN et al., 2016), levando a um maior efeito antibacteriano, mas também a um maior efeito citotóxico, o que muitas vezes limita sua aplicação (KIRMANIDOU et al., 2019; RIAZ AHMED et al., 2017; TAKAMIYA et al., 2016).

O sistema *core-shell* consiste no encapsulamento de íons e drogas e vem sido utilizado para diversas aplicações (HE et al., 2015; NATHANSON et al., 2018; PEREZ; KIM, 2015; TAN et al., 2016). Uma alternativa para eliminar o efeito citotóxico das nanopartículas de prata é aumentar a estabilidade de degradação destas partículas, proporcionando assim um maior controle sobre a liberação de prata pelas mesmas (KASHANI et al., 2020; TAN et al., 2016). A tradução de *core-shell* é “núcleo/casca”, ou seja, estas partículas possuem o “recheio” de um material e uma “casca” de outro. Ao utilizar este sistema podemos combinar propriedades de dois materiais diferentes, entregando à partícula efeitos sinérgicos, reduzindo efeitos colaterais de certas drogas, fornecendo propriedades biocompatíveis ou estabilizando a partícula ativa para que seu efeito seja entregue de forma controlada, aumentando sua eficácia e diminuindo sua toxicidade (KASHANI et al., 2020; TAN et al., 2016; YANG et al., 2016). Sintetizar nanopartículas *core-shell* com uma casca de sílica porosa é uma das maneiras de proporcionar uma liberação sustentada de íons nessas partículas (CHEN et al., 2018; TAN et al., 2016; YANG et al., 2016). Mais estabilidade é esperada na estrutura das nanopartículas *core-shell* de prata pois a casca de sílica atua como uma barreira ao redor dos íons de prata ( $\text{Ag}^+$ ), liberando

os mesmos de forma mais lenta, proporcionando assim o efeito esperado e evitando o efeito citotóxico (ERTEM et al., 2017; TAN et al., 2016).

Ag@SiO<sub>2</sub> já foram sintetizadas com sucesso e a atividade antibacteriana das mesmas foram testadas (ALIMUNNISA; RAVICHANDRAN; MEENA, 2017; DHANALEKSHMI; MEENA, 2014; ISAACS et al., 2017; LIU et al., 2017; TAN et al., 2016). Estudos mostraram atividade antibacteriana contra *E. faecalis* em um irrigante endodôntico contendo Ag@SiO<sub>2</sub> (ERTEM et al., 2017). Sendo assim, o objetivo do estudo foi sintetizar e caracterizar nanopartículas *core-shell* de prata, incorporá-las a um cimento endodôntico resinoso experimental e avaliar a influência das nanopartículas em suas propriedades físico-químicas e biológicas.

## **2 OBJETIVO**

O objetivo deste estudo foi sintetizar e caracterizar nanopartículas *core-shell* de prata (Ag@SiO<sub>2</sub>), incorporá-las em um cimento endodôntico resinoso experimental e avaliar a sua influência e as propriedades físico-químicas e biológicas do material.

## **3 ARTIGO CIENTÍFICO**

Este trabalho de conclusão de curso apresenta-se no formato de artigo científico, escrito na língua inglesa e segue as normas referentes ao periódico International Endodontic Journal.

**Title:** Synthesis of silver core-shell nanoparticles and their influence on an experimental resin endodontic sealer: an in vitro analysis

**Authors:**

Victória Britz Rücker, Dental Materials Department, School of Dentistry. Universidade Federal do Rio Grande do Sul victoriabritz@gmail.com (ORCID: <https://orcid.org/0000-0002-4966-839X>)

Gabriela de Souza Balbinot, Dental Materials Department, School of Dentistry. Universidade Federal do Rio Grande do Sul gabriela.balbinot@ufrgs.br (ORCID: <https://orcid.org/0000-0001-9076-2460>)

Fabício Mezzomo Collares, Dental Materials Department, School of Dentistry. Universidade Federal do Rio Grande do Sul fabricio.collares@ufrgs.br (ORCID: <https://orcid.org/0000-0002-1382-0150>)

Vitaliano Gomes de Araújo Neto, Operative Dentistry Division, Department of Restorative Dentistry, Piracicaba Dental School, University of Campinas vitalianoganeto@gmail.com (ORCID: <https://orcid.org/0000-0002-8227-6179>)

Marcelo Giannini, Operative Dentistry Division, Department of Restorative Dentistry, Piracicaba Dental School, University of Campinas giannini@unicamp.br (ORCID: <https://orcid.org/0000-0002-7260-5231>)

Vicente Castelo Branco Leitune, Dental Materials Department, School of Dentistry. Universidade Federal do Rio Grande do Sul vicente.leitune@ufrgs.br (ORCID: <https://orcid.org/0000-0002-5415-1731>)

**Running title:** Endodontic sealer with Ag@SiO<sub>2</sub>

**Keywords:** Antibacterial Agents; Dental Materials; Nanoparticles; Nanoshells; Root canal sealer; Silver.

**Corresponding author:**

Vicente Castelo Branco Leitune

Dental Materials Department, School of Dentistry. Universidade Federal do Rio Grande do Sul  
Ramiro Barcelos Street, 2492. Porto Alegre – RS. 90.035-003 – Brazil

vicente.leitune@ufrgs.br

Phone: +555133085198



**Conflict of Interest**

The authors have stated that there are no conflicts of interest in connection with this article.

**Acknowledgments**

V.B.R would like to thank the National Council for Scientific and Technological Development for scholarship and G.S.B would like to thank CAPES "Coordenação de Aperfeiçoamento de Pessoal de Nível Superior - Brasil - Finance Code 001-Scholarship".

**Funding Statement**

This study was financed in part by the Coordenação de Aperfeiçoamento de Pessoal de Nível Superior - Brasil (CAPES) - Finance Code 001.

**Ethics Approval Statement and Document and Patient Consent Statement**

Human pulp fibroblasts were used in this study. The patients were fully informed about the project and signed an informed consent approved by the research council board (#41445320.4.0000.5347).

**Role of Authors and Contributors**

**Victória Britz Rücker:** investigation, writing - original draft, data curation, project administration; **Gabriela de Souza Balbinot:** conceptualization, writing - original draft, data curation, formal analysis; **Fabício Mezzomo Collares:** conceptualization, writing - Review & Editing, resources, methodology; **Vitaliano Gomes de Araújo Neto:** writing - Review, methodology; **Marcelo Giannini:** writing - Review & Editing, methodology; **Vicente Castelo Branco Leitune:** conceptualization, supervision, funding acquisition, writing - review & editing, methodology.

## Abstract

**Aim:** To avoid root canal recontamination and endodontic treatment failure, endodontic sealers with antibacterial activity could be an alternative. Silver nanoparticles have antibacterial activity and this study aimed to synthesize Ag@SiO<sub>2</sub> nanoparticles, incorporate them into an experimental endodontic resin sealer, and evaluate their influence on physicochemical and biological properties.

**Methodology:** Ag@SiO<sub>2</sub> nanoparticles were produced using the sol-gel process, based on the Stöber method. The particles were characterized in terms of their chemical structure by Fourier-transform infrared spectroscopy (FTIR), X-ray diffraction (XRD), thermogravimetric analysis (TGA), UV-Vis spectral analysis, scanning electron microscopy, and transmission electron microscopy, where the particle morphology and diameter were analyzed. A dual-cured experimental endodontic resin sealer was formulated using 70 wt% UDMA, 15 wt% GDMA, and 15 wt% BisEMA. The photoinitiators were added separately in two pastes. The Ag@SiO<sub>2</sub> nanoparticles were incorporated into the endodontic sealer at the concentrations of 2.5 wt%, 5 wt%, and 10 wt%, and a control group without nanoparticles was also formulated. The endodontic sealers were evaluated for their flow, film thickness, degree of conversion, softening in solvent, radiopacity, cytotoxicity, and antibacterial activity immediately and after nine months in water storage.

**Results:** Silver was detected in the chemical characterization of Ag@SiO<sub>2</sub> that presented a spheric regular shape and average 683.51 nm ± 93.58 diameter. Sealers presented adequate flow and film thickness while radiopacity values were below the ones required by ISO 6876. All groups underwent softening after immersion in solvent. The 10 wt% groups showed a higher loss of subsurface hardness ( $\Delta$ KHN%). No reduction in cell viability was observed. *E. faecalis* viability in biofilm was reduced in 10 wt% groups after 24 h and 9 months.

**Conclusion:** The addition of 10 wt% Ag@SiO<sub>2</sub> reduced *E. faecalis* viability at immediate and longitudinal analysis while maintaining the physicochemical properties of developed sealers.

## Introduction

The main objective of endodontic treatment, in cases of pulp necrosis or pulp infection, is to eliminate bacteria from the root canal system (Sato *et al.* 2012, Jhajharia *et al.* 2015) with chemo-mechanical preparation debridement and intracanal medications. After the procedure, remaining and persisting bacteria could be viable due to inadequate root canal debridement or incomplete root canal seal (Fukushima *et al.* 1990, Lin *et al.* 1991). The root canal system presents a certain complexity and its cleaning, in some cases, is very difficult (Nair, 2006). Bacteria could remain too in inaccessible parts of the canal, especially in the apical portion. Microorganisms surviving in the root canal system may result in recontamination and treatment failure (Siqueira, 2001).

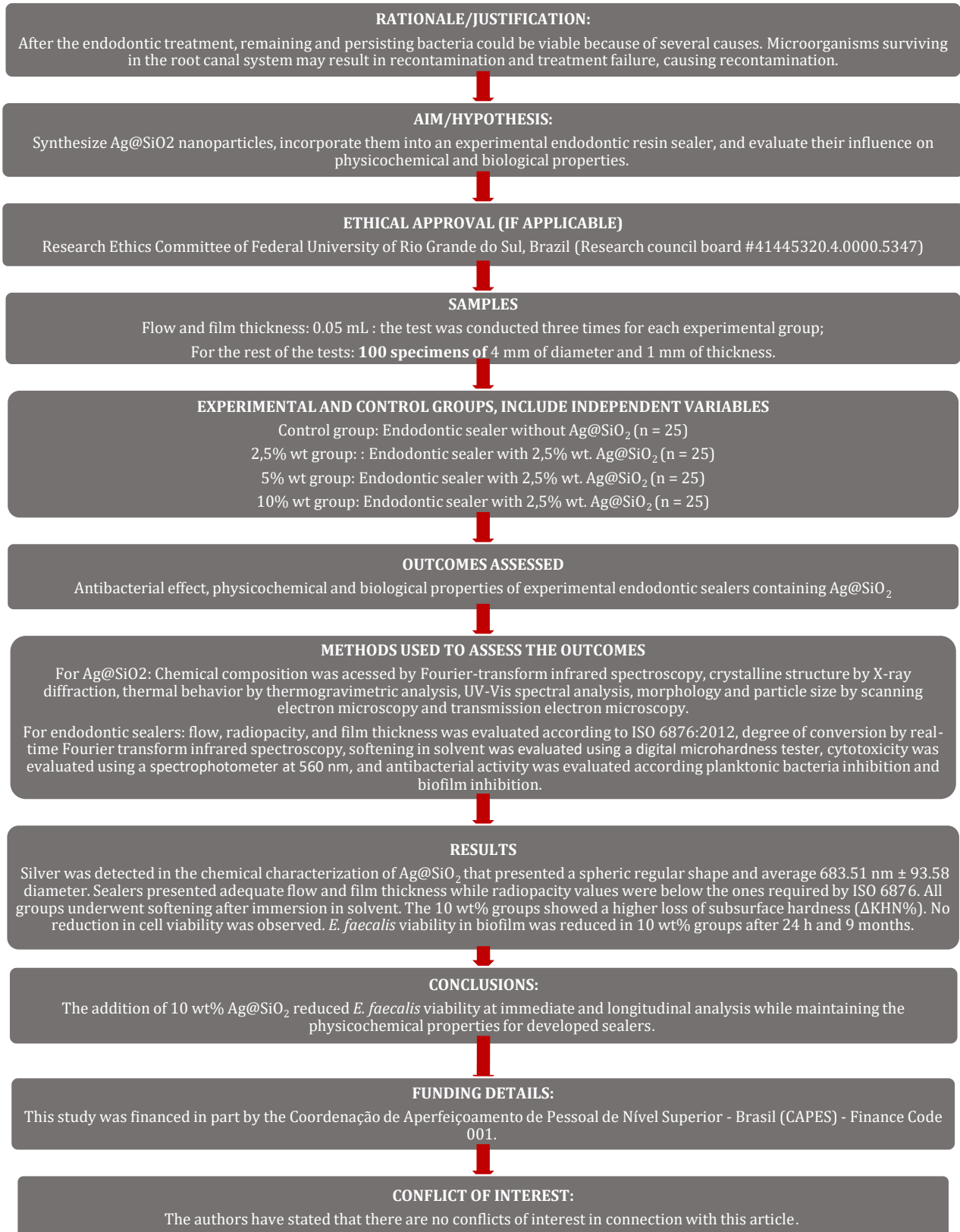
*Enterococcus faecalis* is the most common bacteria in the root canal system after failed root canal treatment (Sundqvist *et al.* 1998) as it can easily penetrate dentinal tubules (Sedgley *et al.* 2005). Several attempts have been made to reduce the viability of *E. faecalis* during and after the endodontic treatment. The incorporation of silver nanoparticles (AgNPs) into root canal sealers has been proposed due to their activity against *E. faecalis* (Corrêa *et al.* 2015, Shrestha & Kishen 2016, Baras *et al.* 2019, Loyola-Rodríguez *et al.* 2019). Previous studies have shown that silver particles interact with the peptidoglycan cell wall (Yamanaka *et al.* 2005) and the constituents of the bacterial membrane causing structural changes and damage to the membranes and intracellular metabolic activity membrane (Jung *et al.* 2008). The particles also interact with bacterial DNA, preventing its replication (Shrivastava *et al.* 2007) and protein synthesis (Yamanaka *et al.* 2005, Shrivastava *et al.* 2007). Silver has historically been used to prevent bacterial infections in several medical devices (Klasen 2000, Silver *et al.* 2006, Cohen *et al.* 2007, Stevens *et al.* 2009). The advancement of nanotechnology allowed the investigation of silver nanoparticles (AgNPs) that also have been widely used as an antimicrobial compound (Corrêa *et al.* 2015, Degrazia *et al.*, 2016, Teixeira *et al.* 2020). The release of oxidized Ag<sup>+</sup> ions becomes greater in AgNPs due to the increased surface area, which leads to a higher amount of active species penetrating the bacterial membrane, resulting

in bacteria death (Dhanalekshmi & Meena 2014, Yang *et al.* 2016, Chen *et al.* 2018). The large surface areas have high responsiveness due to the greater degree of interaction with cells (Tan *et al.* 2016) leading to enhanced antibacterial effect but also higher cytotoxic effect, which often limits their application (Takamiya *et al.* 2016, Riaz Ahmed *et al.* 2017, Kirmanidou *et al.* 2019).

A controlled release of  $\text{Ag}^+$  could be a strategy to reduce the cytotoxicity of these particles. Core-shell nanoparticles have been studied for the encapsulation of ions and drugs for different applications (He *et al.* 2015, Perez & Kim 2015, Tan *et al.* 2016, Nathanson *et al.* 2018) presenting high stability of the particle (Tan *et al.* 2016) and low cytotoxicity (Yang *et al.* 2016). The sustained ions delivery in these particles is achieved by a porous silica shell structure that acts like a barrier (Tan *et al.* 2016, Yang *et al.* 2016, Chen *et al.* 2018), providing a sustained and controlled release of the ion. The potential reduction in cytotoxicity may be related to the dose/response when silver is in contact with living tissues and cells (Shrivastava *et al.* 2007). It is expected that this barrier formed by the silica shell in core-shell structures causes higher stability of the core (Tan *et al.*, 2016). The core-shell system could hamper the rapid release of silver ions and provide higher stability of the  $\text{Ag}^+$ , avoiding possible cytotoxicity and the already known adverse effects related to silver. Previous reports addressed the synthesis of silver core-shell nanoparticles ( $\text{Ag@SiO}_2$ ) (Dhanalekshmi & Meena 2014, Tan *et al.* 2016, Liu *et al.* 2017), and their antibacterial effect against *E. faecalis* was shown when used in endodontic irrigants (Ertem *et al.* 2017). Core-shell silver nanoparticles could, thus, be an alternative for the development of safe antibacterial endodontic resin sealers. The aim of this study was to synthesize  $\text{Ag@SiO}_2$  nanoparticles, incorporate them into an experimental endodontic resin sealer, and evaluate their influence on its physicochemical and biological properties.

## **Materials and methods**

The manuscript of this laboratory study has been written according to Preferred Reporting Items for Laboratory studies in Endodontology (PRILE) 2021 guidelines (Nagendrabadu et al. 2021). Figure 1 is a flowchart of the study design and its outcomes.



\*From: Nagendrababu V, Murray PE, Ordinola-Zapata R, Peters OA, Rôças IN, Siqueira JF Jr, Priya E, Jayaraman J, Pulikkotil SJ, Camilleri J, Boutsoukis C, Rossi-Fedele G, Dummer PMH (2021) PRILE 2021 guidelines for reporting laboratory studies in Endodontology: a consensus-based development. *International Endodontic Journal* May 3. doi: 10.1111/iej.13542. <https://onlinelibrary.wiley.com/doi/abs/10.1111/iej.13542>.

## **Figure 1. Preferred Reporting Items for Laboratory studies in Endodontology (PRILE) 2021 flowchart.**

### **Preparation of core-shell Ag@SiO<sub>2</sub> nanoparticles**

Core-shell nanoparticles were produced based on the Stöber sol-gel process described previously (Dhanalekshmi & Meena 2014). The formation of the silica core was driven by silica condensation in a high pH environment. Tetraethyl orthosilicate (TEOS; Sigma Aldrich, San Luis, Missouri, USA) was slowly mixed in an alcoholic solution (1:3) of ammonium hydroxide (28% NH<sub>4</sub>OH; Neon, São Paulo, Brazil) under stirring at room temperature. This mixture was kept at room temperature for 24 hours. The silver was added to an aliquot of the colloid solution in a water-ethanol solution containing 0.03 mMol of silver nitrate (AgNO<sub>3</sub>; Neon, São Paulo, Brazil). Formaldehyde (Dinamica, São Paulo, Brazil) was used in an aqueous solution (1:5) and added dropwise for stabilization. After 30 min of stirring, the sol was stored for one day, and the particles were washed with water three times. Finally, particles were dried at 60 °C for one day to remove the water.

### *Characterization of core-shell Ag@SiO<sub>2</sub> nanoparticles*

The characterization of particles was conducted considering silica nanoparticles as control. These particles were produced as described above, but no silver precursor was used in this case.

### **Chemical composition**

The chemical composition of Ag@SiO<sub>2</sub> particles was assessed by Fourier transform infrared spectroscopy. The particle powder was compressed on top of the diamond crystal of an attenuated total reflectance (ATR) device (Platinum ATR-QL; Bruker Optics) at a spectrometer (Vertex 70; Bruker Optics, Ettlingen, Germany) directly, without mixture in KBR

or any solvent. The analysis was performed in the range of 4000 to 400  $\text{cm}^{-1}$  and 64 scans with a 4  $\text{cm}^{-1}$  resolution.

### **Crystalline structure**

The crystalline structure of  $\text{Ag@SiO}_2$  particles was assessed with X-ray diffraction (X'PertPRO, PANalytical MPD, Netherlands) using  $\text{CuK}\alpha$  radiation at 40 kV – 40 mA at an angular range between  $5^\circ$  e  $100^\circ$ , with a step size of  $0.02^\circ$  during 5 s.

### **Thermogravimetric Analysis**

A thermogravimetric analyzer (TGA Discovery; TA Instruments, New Castle, DE, USA) was used to assess the thermal behavior of  $\text{Ag@SiO}_2$ . The nanoparticles were weighed ( $0.2\text{g} \pm 0.01$ ) and heated in a platinum pan up to  $800^\circ\text{C}$  at a rate of  $20^\circ\text{C} \cdot \text{min}^{-1}$  under nitrogen purge ( $25 \text{ mL} \cdot \text{min}^{-1}$ ). The % weight loss (TGA) and the differential thermogravimetric (DTG) were calculated to compare the thermal behavior and the derivative weight loss, respectively for particles with and without silver.

### **UV-Visible Spectral**

UV–Visible spectra were analyzed in a spectrophotometer (Spectronic 21D; Milton Roy, PA, USA) by the relative absorbance in a wavelength range between 200-500 nm. Distilled water was used as a reference for the analysis. A 0.05 mg/ml particle concentration was used for the analysis and the absorbance curves were plotted with Gaussian curve fitting.

### **Morphology**

For the scanning electron microscopy (SEM), the particles were placed on an aluminum sample holder and gold-coated before the analysis under 10 kV (Jeol JSM-6060 Germany). Transmission electron microscopy (TEM) was performed with a dispersion of particles into propanol at 5 wt%. This solution was then dispersed on a square 400-mesh copper grid (TEM: Electron Microscopy Sciences, Hatfield, PA, USA) and analyzed using TEM (JEM 1400; Jeol, Tokyo, Japan) at 80 kV at X25k, X40k, and X60k magnifications.

## **Particle diameter**

The size of the particles was measured on the SEM images. The measurement was performed on three images at 30x magnification. Fifty samples randomly chosen were measured at each image, and the average diameter was recorded. The images were measured at ImageJ (NIH, Maryland, USA).

### *Formulation of the experimental endodontic resin sealers*

The dual-cured experimental endodontic resin sealers were formulated with urethane dimethacrylate (UDMA) at 70 wt%, glycerol 1,3-dimethacrylate (GDMA) at 15 wt% and ethoxylated bisphenol-A glycol dimethacrylate (BisEMA) at 15 wt%. As a dual system, the photoinitiators were added separately in two different pastes. Camphorquinone (Sigma Aldrich, San Luis, Missouri, USA) and dihydroxy ethyl-para-toluidine (DHEPT; Sigma Aldrich, San Luis, Missouri, USA) were added in Paste A. Benzoyl peroxide (Sigma Aldrich, San Luis, Missouri, USA) was used in Paste B. Barium glass with 454 m<sup>2</sup>/g of surface area and 1.3 µm of particle size (Esstech; Essington, PA, USA) was added to both pastes as filler, at 10 wt% concentration. Ag@SiO<sub>2</sub> nanoparticles were incorporated into the experimental sealers at 2.5 wt%, 5 wt%, and 10 wt%. Sealers without Ag@SiO<sub>2</sub> were used as a control group.

### *Characterization of experimental endodontic sealers*

#### **Flow**

The flow test was conducted according to ISO 6876:2012 (Standardization 2012). The experimental endodontic resin sealer was placed on a glass plate (40 x 40 x 5 mm; 0.05 mL) with a graduated 1.5 mL syringe. At 180 ± 5 s after mixing a second plate (20 ± 2 g) was placed on top of the sealer with a 100 g load for 10 min. The major and minor diameters of the compressed material were measured using a digital caliper. The test was conducted three times for each experimental group, and the mean value was recorded.

#### **Film thickness**



The film thickness was evaluated according to ISO 6876:2012 (Standardization 2012). The thickness of two glass plates (5 mm in thickness x 10 mm in length; n = 3) was initially measured. The experimental sealers were placed in the center of one plate (0.05 mL) and, after  $180 \pm 5$  s mixing, the second plate covered the sealer. A 150 N load was applied for ten minutes and the plate thickness was measured again. The difference in the thickness of the plates, with and without the sealer, was recorded.

### **Degree of conversion**

The degree of conversion (DC) of the experimental endodontic resin sealers was evaluated using real-time Fourier transform infrared spectroscopy (RT-FTIR) with a Vertex 70 (Bruker Optics, Ettlingen, Germany) spectrometer equipped with an attenuated total reflectance device composed of a horizontal diamond crystal with a mirror angle of 45 degrees. Support was coupled to the spectrometer to fix the light-curing unit and standardize the distance of 1 mm from the top of the specimens. The samples (n=3) were evaluated before, immediately after, and 7 days after the photoactivation. The samples were light-cured for 40 s (RadiiCal, SDI, Bayswater, Vic., Australia). Opus software (Bruker Optics) was used in the monitoring scan mode, with Blackman-Harris 3-Term apodization in a range of  $4000\text{--}400\text{ cm}^{-1}$  and resolution of  $4\text{ cm}^{-1}$ . With this setup, one spectrum was obtained before photocuring, and one immediately after photocuring. The degree of conversion was calculated as described in a previous study (Collares *et al.* 2011), considering the intensity of carbon-carbon double bond stretching vibration (peak height) at  $1635\text{ cm}^{-1}$ , and using the carbonyl group at  $1720\text{ cm}^{-1}$  from the polymerized and unpolymerized samples as an internal standard (Stansbury & Dickens 2001).

### **Softening in solvent**

The softening of the developed endodontic sealer was evaluated with three specimens per group (n = 3; 4 mm of diameter and 1 mm of thickness). Sealers were photoactivated for 40 s and polished using SiC abrasive papers (granulation of 600, 1200, 2000) under

continuous irrigation (distilled water), and finally finished using a felt disc embedded with aluminum oxide suspension (0.05  $\mu\text{m}$ ). The Knoop microhardness was evaluated using a digital microhardness tester (HMV-2, Shimadzu, Tokyo, Tokyo, Japan). Three indentations (10 g/5 s) were performed on the surface of each specimen to determine the initial Knoop hardness number (KHN1). Subsequently, the specimens were stored for 2 h in a solution containing ethanol and water (50 vol.% – 50 vol.%) and the final Knoop hardness (KHN2) was assessed. The percentage difference (softening ratio) between KHN1 and KHN2 was calculated ( $\Delta\text{KHN}\%$ ) for each group.

### **Radiopacity**

Radiopacity was evaluated with sixteen specimens ( $n = 4$ ) with 10 mm ( $\pm 0.5$  mm) diameter, and 1 mm ( $\pm 0.2$  mm) thickness was used and tested according to ISO 6876:2012 (Standardization 2012). A digital system with a phosphor plate (VistaScan; Durr Dental GmbH & Co. KG, Bietigheim-Bissingen, Germany) was used. X-ray equipment operating at 70 kV and 8 mA, for 0.4 s of exposure time and a focus distance of 400 mm was used. An aluminum step wedge was used in every image (ISO 6876:2012). The images were converted to .tiff and analyzed with ImageJ 1.48d (Wayne Rasband, National Institutes of Health, USA) software, and the density of pixels was converted to aluminum millimeters (mmAl).

### **Cytotoxicity**

Human pulp fibroblasts were collected from third molars of patients who had indicated therapeutic extraction. These patients were fully informed about the project and signed an informed consent approved by the research council board (#41445320.4.0000.5347). Cytotoxicity was evaluated with five specimens per group ( $n = 5$ ) with 1 mm of thickness and 4 mm of diameter immersed in 1 mL of Dulbecco's Modified Eagle Medium (DMEM) for 24 h for eluates preparation. Pulp fibroblasts were placed at  $5 \times 10^3$  per well in a 96-well plate with 100  $\mu\text{L}$  of DMEM with the eluate previously prepared. Besides that, cells were too cultivated in independent wells with pure DMEM media to assess their behavior without any material

influence. After 72 h, the cells were fixed with trichloroacetic acid at 10% and incubated at 4 °C for 1 h, washed six times with running water, and dried at room temperature. Sulforhodamine B at 0.4% was added to stain the cells, and the plate was incubated for 30 min at room temperature. The plates were washed four times with acetic acid at 1% and dried at room temperature. Trizma solution was added, and the plate was incubated for 1 h to allow complete solubilization of the dye. The microplates were analyzed in a spectrophotometer at 560 nm. The absorbance found in wells with cells treated with pure DMEM was used to normalize the values observed in wells treated with developed sealers.

### **Antibacterial activity**

The antibacterial analysis was conducted to assess the reduction in colony-forming units (CFU) of *E. faecalis* (INCQS 00234, ATCC 29212) in two distinct situations: in the ability to reduce the adhesion of bacteria to the material surface for biofilm formation and in the ability to reduce the planktonic bacteria. The sealers with Ag@SiO<sub>2</sub> addition were tested along with the core-shell-free materials (Control). For the planktonic analysis, a suspension of *E. faecalis* that was not in contact with any material was used as a negative control. The analysis was conducted immediately after sample production and storage in water for 24 h at 37 °C. A longitudinal analysis was performed with samples that were stored in the same conditions for nine months.

### **Biofilm inhibition**

Five specimens per group (n = 5) were prepared (4 mm diameter; 1 mm thickness). The specimens were attached to the lid of a test plate, and the assembly was submitted to sterilization by hydrogen peroxide plasm. Each well of the test plate was inoculated with 900 µL of brain-heart infusion (BHI) broth and 100 µL of a suspension of an overnight broth culture of *E. faecalis* corresponding to  $9.2 \times 10^8$  CFU/mL. The lid with the specimens was placed on the sterile well-plate, and the surfaces of the specimens were exposed to the BHI broth with the bacteria at 37 °C for 24 h. The specimens were removed from the lid and vortexed in 1 mL

of saline solution (0.9%) for 1 min to be subsequently diluted until  $10^{-6}$  dilutions. Two 25  $\mu\text{L}$  drops of each dilution were plated in BHI-agar Petri dishes and incubated at 37 °C for 48 h. The number of colony-forming units (CFUs) was visually counted and transformed to log CFU/mL.

#### Planktonic bacteria inhibition

Five specimens per group ( $n = 5$ ) with 4 mm of diameter and 1 mm of thickness were prepared, attached to the lid of a test plate, and submitted to sterilization by hydrogen peroxide plasm. Each well of the test plate was inoculated with 900  $\mu\text{L}$  of brain-heart infusion (BHI) broth and 100  $\mu\text{L}$  of a suspension of an overnight broth culture of *E. faecalis* corresponding to  $9.2 \times 10^8$  CFU/mL. The lid was placed on the sterile well plate, where the surfaces of the specimens were exposed to the bacteria-containing BHI broth at 37 °C for 24 h. For the first dilution, 100  $\mu\text{L}$  of each well was diluted in 900  $\mu\text{L}$  of saline solution, and the solutions were diluted until  $10^{-6}$ . Three wells containing BHI and 100  $\mu\text{L}$  of the suspension of an overnight broth culture of *E. faecalis* were used as the negative control. Two drops of 25  $\mu\text{L}$  each from each dilution were plated in BHI agar on Petri dishes and incubated for 48 h at 37 °C to visually count and calculate the log CFU/mL.

#### *Statistical analysis*

Normality of data was assessed by Shapiro-Wilk while homoscedasticity was evaluated with Levene's test. One-way ANOVA and Tukey *post hoc* test was used to compare KHN1, %KHN, radiopacity, flow, film thickness, antibacterial activity against biofilm formation, antibacterial activity against planktonic bacteria, and cytotoxicity. Two-way ANOVA and Tukey were used to analyze the degree of conversion and antibacterial analysis data. The paired *t*-test was used for comparison between the initial and final Knoop microhardness in ethanol softening. All tests were performed at 95% significance.

## **Results**

Figure 2 shows FTIR spectra and XRD diffractograms for Ag@SiO<sub>2</sub> particles. Figure 2a shows the peak at 1050 cm<sup>-1</sup> as the shift of the Si-O-Si bond (1090 cm<sup>-1</sup>), related to the presence of Ag on the nanoparticles. In the XRD analysis, an amorphous structure is observed for pure silica nanoparticles, while the crystal structure on Ag@SiO<sub>2</sub> shows the presence of face-centered cubic structure (CFC) on the peaks assigned to the 111, 200, and 220 crystal planes (Figure 2b). TGA and DTG analyses are shown in Figure 2c,d. An initial weight loss is found until 100 °C for both particles, which may be related to residual solvent degradation, while marked differences are observed after the temperature reaches 200 °C. While a characteristic silica weight loss is found in the nanoparticles, a major degradation of Ag@SiO<sub>2</sub> takes place from 220 °C to 300 °C which may be assigned to the loss of core-shell structure. Both particles were not fully degraded with up to 80 wt% of reminiscent mass after 800 °C. SEM and TEM images in different magnifications are shown in Figure 3. Spherical and organized particles were observed, and the distribution of particle diameter showed that the average diameter of synthesized particles was 683.51 ± 93.58 nm. The TEM ultramorphology of the nanoparticles synthesized in this study is depicted in Figure 3d-f. Spherical particles were observed with a dark gray shell and a darker core structure as observed in Figures 3e and f. Disperse structures were observed within the particles, and on the external surface of cores, as well. The UV-Vis absorption curves are shown in Figure 3h. A shift in the reduction peak from pure silica particles to the Ag@SiO<sub>2</sub> ones is observed and later presents a main absorption at the characteristic silver peak, at 405 nm.

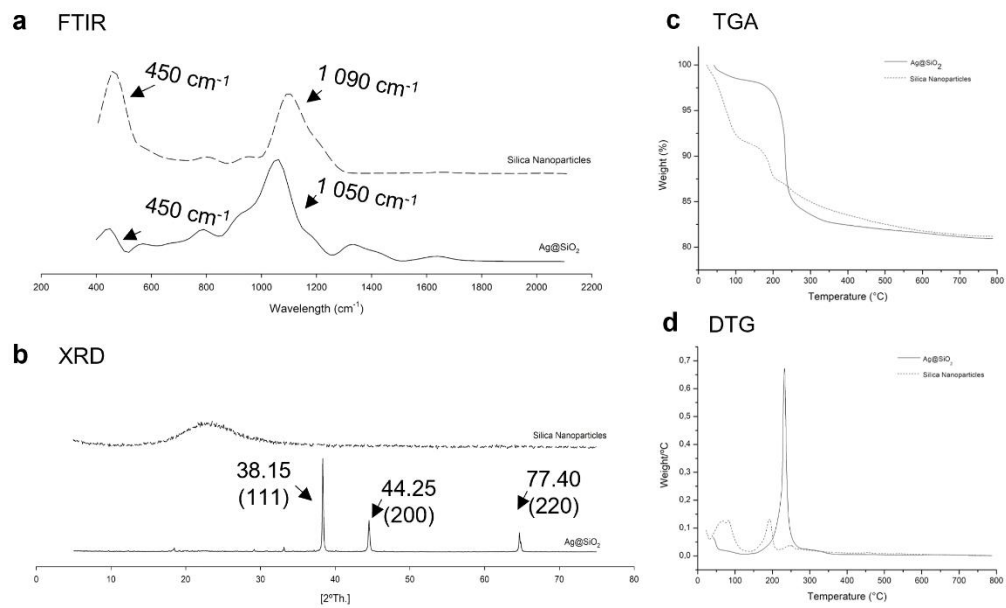


**Figure 2. Silver core-shell nanoparticle chemical characterization.** The chemical composition was assessed by the Fourier transform infrared (FTIR) spectra (a), where the shift in the Si-O peak is assigned to the presence of Ag in the particle structure. XRD diffractograms (b) of the Ag@SiO<sub>2</sub> particles show the presence of crystalline structures of silver compounds. TGA and DTG curves also show thermal degradation around  $\sim 250^{\circ}\text{C}$ , which is assigned to the presence of chemical components in the silica structure (c, d).

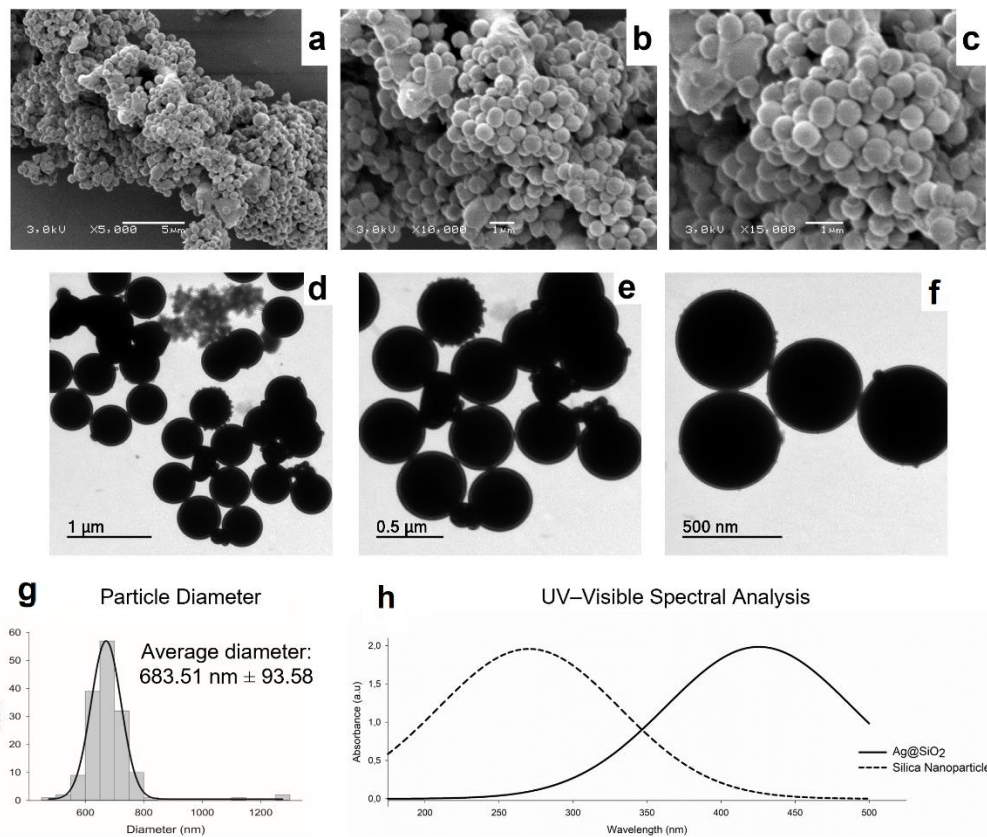


**Figure 3. Core-shell nanoparticle morphology and particle size.** SEM characterization of core-shell nanoparticles morphology in 5000x (a), 10000x (b) and 15000x (c) magnification. (d-f) TEM images were showing the core-shell structure and deposition of structures on the outer surface of nanoparticles. Spherical particles were observed. The distribution of particle size is shown in d and the average diameter was  $683.51 \pm 93.58$  nm. The UV-Vis absorption curves (e) present a shift in the reduction peak from pure silica particles to the Ag@SiO<sub>2</sub>, indicating the modification in the particles with the incorporation of silver in the synthesis.

The results of radiopacity, flow, film thickness and DC are shown in Table 1. For radiopacity, there was no significant difference between groups ( $p > 0.05$ ), and all the tested groups obtained values below the requirements by ISO 6876:2012. The flow values ranged from  $24.00 \pm 3.12$  mm to  $32.66 \pm 2.02$  mm, and all groups reached values according to ISO 6876:2012. All groups exhibited films of thickness up to 50 μm, with no significant difference between groups ( $p > 0.05$ ). The values of immediate DC ranged from  $60.86 \pm 5.03\%$  for the 5

wt% groups to  $40.82 \pm 17.84$  for 10 wt%. After seven days, no statistically significant differences were found ( $p > 0.05$ ).

**Table 1** - Mean and standard deviation values of flow (mm), film thickness (mm), radiopacity (mmAl), and degree of conversion (DC%) for experimental endodontic resin-based sealers.

Groups	Flow (mm)	Film thickness (mm)	Radiopacity (mmAl)	DC (%)	
				Immediate	24H
<b>Control</b>	$24.00 \pm 3.12^B$	$6.67 \pm 5.77^A$	$1.28 \pm 0.28^A$	$58.63 \pm 5.03^{aA}$	$63.92 \pm 9.94^{aA}$
<b>2.5 wt%</b>	$31.50 \pm 2.64^A$	$13.33 \pm 5.77^A$	$1.60 \pm 0.22^A$	$47.25 \pm 7.75^{aA}$	$52.05 \pm 7.78^{aA}$
<b>5 wt%</b>	$32.66 \pm 2.02^A$	$6.66 \pm 5.77^A$	$1.43 \pm 0.44^A$	$60.86 \pm 5.03^{aA}$	$61.34 \pm 4.54^{aA}$
<b>10 wt%</b>	$28.16 \pm 1.52^{AB}$	$13.33 \pm 5.77^A$	$1.33 \pm 0.29^A$	$40.82 \pm 17.84^{aA}$	$40.89 \pm 21.24^{aA}$

Different capital letters indicate a statistically significant difference in the same column ( $p < 0.05$ ).

Different small letters indicate a statistically significant difference in the same row ( $p < 0.05$ ) for the same test.

The results of Knoop microhardness and softening ratio are shown in Figure 4. The KHN1 results ranged from  $16.37 \pm 0.65$  for the 2.5 wt% group to  $18.57 \pm 1.13$  for the 10 wt% group. A decrease in Knoop microhardness was observed after immersion in the solvent for all groups ( $p < 0.05$ ). The 10 wt% group showed greater  $\Delta$ KHN% than the control group and 5 wt% group ( $p < 0.05$ ). No statistically significant difference was observed for the 2.5 wt% group when compared to the other ones ( $p > 0.05$ ).

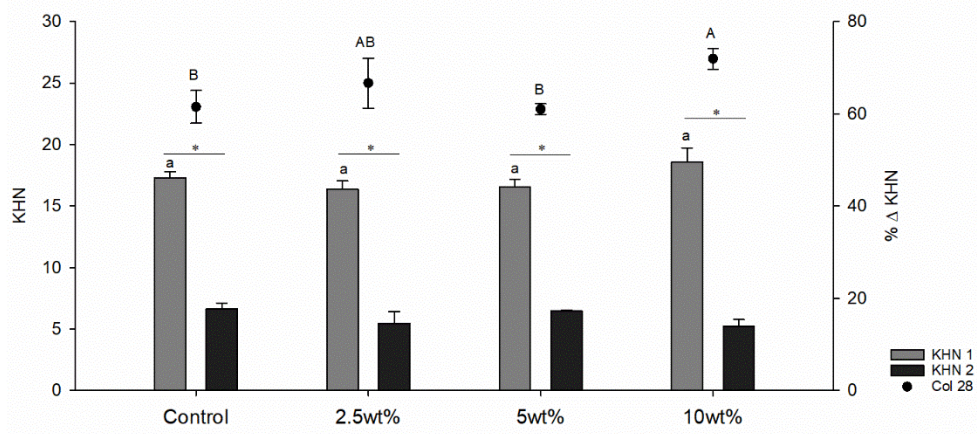




**Figure 4. Knoop microhardness and softening ratio results.** The KHN1 results ranged from  $16.37 \pm 0.65$  for the 2.5 wt% group to  $18.57 \pm 1.13$  for the 10 wt% group. A decrease in Knoop microhardness was observed after immersion in the solvent for all groups ( $p < 0.05$ ). The 10 wt% group showed greater  $\Delta$ KHN% than the control group and 5 wt% group ( $p < 0.05$ ). No statistically significant difference was observed for the 2.5 wt% group when compared to the other ones ( $p > 0.05$ ).

The results of cytotoxicity and antibacterial activity are shown in Figure 5. The cell viability of all groups was normalized with the viability of cells in wells without the eluate. No reduction of cell viability was observed with the addition of up to 10 wt% of Ag@SiO<sub>2</sub>. These values ranged from  $112.32 \pm 3.61\%$  for the control group to  $102.87 \pm 5.14\%$  for the 10 wt% group, with no significant difference between the groups (Figure 5a;  $p > 0.05$ ). The viability of *E. faecalis* was reduced for the 10 wt% concentration in immediate and longitudinal analysis (Figure 5b), with no statistically significant difference between the time points. An increase in the bacterial viability was found in control samples after nine months of storage, while the 2.5 wt% and 5 wt% concentrations presented a reduction in the Log CFU/ml from the 24 h to the 9-month analysis (Figure 5b;  $p < 0.05$ ). No statistical differences were found between groups for bacterial viability in planktonic analysis, regardless of the group or time point of analysis (Figure 5c;  $p > 0.05$ ).

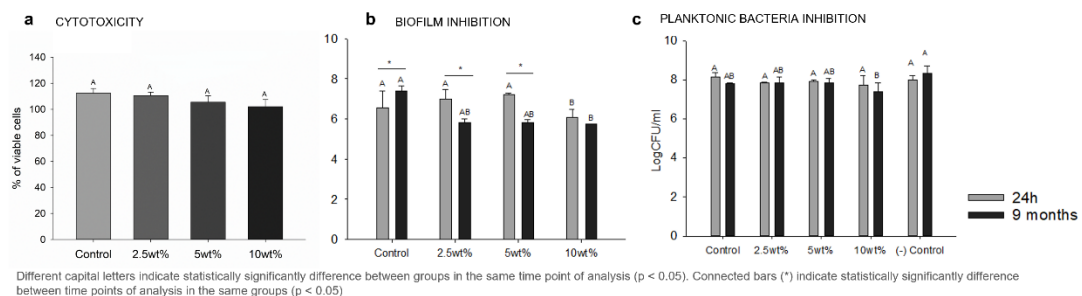


**Figure 5. Cytotoxic analysis and antibacterial activity.** The percentage of viable cells is shown in (a), no reduction of cell viability was observed with the addition of up to 10 wt% of Ag@SiO<sub>2</sub>. Mean and standard deviation values of direct contact inhibition assay (b) and

planktonic bacteria inhibition (c) assay in colony-forming units per milliliter with the logarithmic transformation (log CFU/mL), after 24-h and 9-month analysis. The viability of *E. faecalis* was reduced for the 10 wt% concentration in immediate and longitudinal analysis (b). No statistical differences were found between groups for bacterial viability in planktonic analysis, regardless of the group or time point of analysis (c).

## Discussion

The addition of antibacterial agents in the composition of endodontic sealers may be used as a strategy to decrease the risk of recontamination of the root canal system after endodontic treatment (Barros *et al.* 2014). The development of sealers with antibacterial ability has been studied (Bodrumlu & Semiz 2006, Slutzky-Goldberg *et al.* 2008, Zhang *et al.* 2009), and the use of silver as an antibacterial particle has been proposed (Zhao *et al.* 2011, Roguska *et al.* 2012). In the present study, silver core-shell nanoparticles with antibacterial potential were produced. The addition of these particles to resin-based root canal sealers did not influence the physicochemical properties or the biocompatibility. The 10 wt% concentration promoted a reduction in *E. faecalis* viability in the biofilm that was maintained during up to nine months of storage.

The formulation of Ag@SiO<sub>2</sub> nanoparticles was based on the Stöber method (Stöber, Fink and Bohn, 1968), and the control in shape and size was accomplished in the present study as observed on SEM analysis (Figure 3), where the size was measured, showing an average of 683.51 nm diameter. The nanosized structure of these particles may contribute to the release of compounds, such as antibacterial agents (Liu *et al.* 2017, Dhanalekshmi *et al.* 2019, Guo *et al.* 2019) and other drugs (He *et al.* 2015, Yang *et al.* 2016). The presence of Ag as the core of the nanoparticles is suggested by the results found in, XRD, FTIR, TGA, and TEM, UV-Vis analysis. In the XRD, the presence of crystalline silver in the structure is observed and the shift in the silica characteristic peak (from 1090 cm<sup>-1</sup> to 1050 cm<sup>-1</sup>) in the FTIR is assigned to the presence of chemical components in the silica structure (Guo *et al.* 2019, Feng *et al.* 2019). TGA and DTG curves also show thermal degradation around ~250 °C (Figure 2c,d). Ag<sup>+</sup> ions

are reported to degrade around 400 °C in AgNPs (Rajasekharreddy & Rani 2014, Rodrigues *et al.* 2020), while here the interaction of silver and silica may have lowered the temperature, which was previously found in silica-inorganic interactions (Rodrigues *et al.*, 2020). TEM showed the presence of a well-defined dark gray spherical shell structure, which may be assigned to the silica that is organized surrounding a darker core, probably composed of Ag compounds (Figure 3d-f). These findings suggest that Ag was successfully incorporated into silica-shell nanoparticles, while it may also be found adsorbed on the outer surface of spheres. These findings corroborate the chemical analysis shown in Figure 2 and the shift in UV-Vis absorbance from the silica regions (~220 nm) to the silver region (405 nm), that also indicates the modification in the particles with the incorporation of silver in the synthesis, which was previously found for different silver-containing antibacterial particles (Zhao *et al.*, 2011; Singh, Kim and Yang, 2016; Videira-Quintela *et al.*, 2020). As a single type of particle is observed in SEM analysis, the silver observed in the characterization is likely confined in the core of the particles thus, evidencing the formulation of a core-shell particle.

The maintenance of regular particle size and morphology is essential to maintain the application of these particles as inorganic fillers (Feng *et al.* 2019) and the physicochemical properties of developed composite materials. The developed core-shell nanoparticles were incorporated into the endodontic resin-based sealer, and none of the tested concentrations modified the film thickness ability for the developed sealers, while modifications were observed at up to 2.5 wt% Ag@SiO<sub>2</sub> addition in the flow results (Table 1). The flow values were higher than 17 mm, and the film thickness was lower than less than 50 mm, as required for endodontic sealers by ISO 6876: 2012 (Standardization 2012). Due to these specific characteristics, the formulated sealers are potentially able to reach the apical foramen and penetrate the entire root canal system, which has small irregularities and ramifications (Siqueira *et al.* 1995). These could be an important property for these sealers if the antibacterial activity is considered, as the bacteria that reach the root canal system can adhere to dentine walls and dentinal tubules (Ando & Hoshino 1990), and this area must be disinfected as well. The addition of inorganic

fillers could influence these properties by increasing the viscosity of resin-based materials but the addition of Ag@SiO<sub>2</sub>, in the concentrations of the groups tested, was able to maintain the flow and film thickness, as shown in Table 1. This may be explained by the fact that other characteristics besides concentration, like the size of the particle and characteristics of the shell in the case of core-shell nanoparticles, are important to determine the increase or not of the properties like flow and film thickness (Benhadjala, Gravouelle and Bord-Majek, 2015; Habib, Wang and Zhu, 2018). Another explanation could be the fact that the concentration of nanoparticles added was not enough to increase the viscosity of the sealer. Although these properties are following ISO 6876 requirements (Standardization 2012) the radiopacity did not reach the 3 mmAl required by the standard. As the Ag@SiO<sub>2</sub> did not promote adequate values and it could be a limitation of the sealer, the addition of radiopacifiants could be considered (Collares *et al.* 2010, Leitune *et al.* 2013).

The proper sealing of the root canal system depends on the appropriate formation of the polymeric matrix, maintaining the stability of the sealer after obturation (Drummond, 2008). The degree of conversion was evaluated because insufficient polymer conversion could affect the properties of the endodontic sealers. The low degree of conversion is associated with a low bond strength, higher cytotoxicity, and higher softening in solvent (Lee *et al.*, 2011), causing a decrease in mechanical properties of the resin-based materials (Ferracane, 1985; Collares *et al.*, 2011). The degree of conversion (Table 1) showed no statistically significant difference ( $p > 0.05$ ) between the groups during the immediate and seven days of analysis. No statistically significant difference was observed within the different concentrations as well. It is expected that the dark yellow color found for the particles would lead to a reduction in light passage throughout the materials because an increase of the fillers could reduce the DC in the experimental root canal sealers (Howard *et al.*, 2010; Belli *et al.*, 2014), but the presence of up to 10 wt% Ag@SiO<sub>2</sub> did not influence the polymerization of sealers, as observed in Table 1. Although not statistically significant, the 10 wt% group showed a reduction in DC, but the

results remain similar to those methacrylate-based commercially available endodontic sealers (Rostirolla *et al.*, 2019).

As said before, the color of materials containing Ag<sup>+</sup> in their composition could be considered an issue because of the decrease in polymerization and because of the possibility of causing a stain in the tooth. Studies that analyzed the stain caused by sealers placed it in the pulp chambers rather than the root canal, resulting in changes in tooth color and unsatisfactory esthetic results (Chakmakchi *et al.*, 2020). In addition, the silver-containing dental materials that were tested had free silver in their formulation. Because the sealers formulated in this project contain a core-shell nanoparticle, a sustained release of ions is expected due to the porous structure of the silica shell (Singh, Kim and Yang, 2016; Tan *et al.*, 2016; Chen *et al.*, 2018), decreasing the adverse effects of silver release in the material.

While the degree of conversion is responsible for evaluating the carbon double bonds conversion of the aliphatic portion on methacrylate-based materials, the softening rate in the solvent is an indicator of the stability of the polymer network. A material with a low degree of conversion or with inadequate polymerization can be more easily encroached by solvents (Pearson and Longman, 1989; da Silva *et al.*, 2008; Collares *et al.*, 2011), and this can explain the fact that the 10 wt% group, with a lower degree of conversion, also presented the greater softening rate in solvent. The solvent affects the cross-linking density and a structure more prone to solvent absorption may be more likely to undergo a faster hydrolytic degradation (Collares *et al.*, 2011). When the samples are immersed in ethanol the forces of attraction between solvent molecules and components of the chains are bigger than the forces of attraction of polymer chains. This attraction makes the polymeric network swell and makes the solvent penetrate the resin matrix (Ferracane 2006). The absorption of solvents, such as the alcoholic solution used in this study, by the sealer produces a relaxation process that leads to a separation of the polymer chains (Ferracane, Berge and Condon, 1998), decreasing the mechanical properties of the polymer (Ferracane, 2006) and its hardness. The 10 wt% Ag@SiO<sub>2</sub> group showed the highest softening rate in the solvent, and this result was

statistically different from the control group ( $p < 0.05$ ). The addition of fillers can lead to degradation of the material due to fluid infiltration, gap formation, and leaching of monomers. This is an inherent limitation of the study because of the decrease in the properties of the sealer with the addition of 10 wt% Ag@SiO<sub>2</sub>.

Unreacted monomers and degradation products are known to be responsible for cytotoxic effects on dental materials (Michelsen *et al.* 2008, Al-Hiyasat *et al.* 2010), and silver nanoparticles are shown to increase cell death (Marin *et al.* 2015). The potential cytotoxicity of silver nanoparticles is shown for different applications (Abbasi *et al.* 2016), but little is known about the cytotoxicity effect when silver nanoparticles are incorporated into endodontic materials (Chávez-Andrade *et al.* 2017, Teixeira *et al.* 2020). Since endodontics sealers closely contact the periapical tissues, fibroblast cells were used for this test. The cytotoxic potential of endodontic sealers, along with the inflammatory response that is often present in the periapical tissues due to the endodontic treatment, can increase tissue damage, inhibiting or delaying the healing process (Silva *et al.* 2014). Silver nanoparticles were tested in commercial resin-based sealers and root canal irrigants, and in both cases, the incorporation of these nanoparticles reduced the viability of fibroblasts (Chávez-Andrade *et al.* 2017, Teixeira *et al.* 2020), which was not observed in the present study ( $p > 0.05$ ; Figure 5). A strategy to reduce the potential cytotoxicity of these nanoparticles is the self-assembled Ag@SiO<sub>2</sub> that could promote a controlled delivery of Ag<sup>+</sup> without promoting toxicity (Ertem *et al.* 2017). The assembled structure of core-shell nanoparticles and the adequate formation (Figure 3) of the polymeric network, in this case, could be related to reduced cell death in up to 10 wt% Ag@SiO<sub>2</sub> sealers. The cytotoxic effect on silver-containing materials is related to the concentration of this compound in the materials (Ai *et al.* 2017, Chávez-Andrade *et al.* 2017), and the proper balance between the antibacterial activity and the toxicity must be achieved (Marin *et al.* 2015).

The silver nanoparticles release oxidized Ag<sup>+</sup> ions that are the active species that penetrated the bacterial membrane, resulting in cell death (Yang *et al.* 2016, Dhanalekshmi *et*

*al.* 2019, Feng *et al.* 2019). The release of these ions was shown previously in free silver nanoparticles with effective antibacterial activity against *Enterococcus faecalis* (Sofi *et al.*, 2012). Ag@SiO<sub>2</sub> nanoparticles were also shown to provide the antibacterial effect to irrigants for endodontic applications (Ertem *et al.* 2017), where the antibacterial effect was observed immediately and maintained up to 168 h after the initial contact with *E. faecalis* biofilm. This sustained drug release is expected for these particles as the core structure made of silica is not a continuous capsule (Dhanalekshmi & Meena 2014), and the release of these active species could occur smoothly through the core pores (Ertem *et al.* 2017). The obtained structure for the Ag@SiO<sub>2</sub> (Figure 2 and Figure 3) and the possible presence of Ag<sup>+</sup> ions in the 10 wt% concentration were shown to reduce the *E. faecalis* viability after 24 h and 9 months (Figure 5b, c). The duration of interaction also defines the nanoparticle's ability to disinfect the root canal (Kishen *et al.* 2008, Wu *et al.* 2014), and in this case, a long-term antibacterial activity was identified. Although the 2.5 wt% and 5 wt% concentrations presented intermediate behavior when compared to control and 10 wt%, the longitudinal analysis showed a reduction in Log CFU/ml when compared to the immediate, showing that the release of Ag<sup>+</sup> ions could be taking place over time as the polymeric and particle degradation takes place. That release of Ag<sup>+</sup> ions over time is the strength of the study and this particularity should be further explored. In this study, we could not demonstrate how the controlled silver release occurs and it can be seen as a limitation.

The balance between the antibacterial activity of silver and the effect of these nanoparticles on the physicochemical and biological properties is a challenge for composite materials in Dentistry. In the present study, Ag@SiO<sub>2</sub> was synthesized, and the addition of up to 10 wt% did not affect the biocompatibility of experimental endodontic sealers and showed an immediate and long-term antibacterial effect. Although the reduction in CFU count in the 10% group is statistically significant, it is not desired because it is less than 2 log. Nevertheless, the result represents an antibacterial activity and is relevant, mainly because antibacterial activity was also present in the 9-month analysis, indicating that there is a sustained release

of silver by the material. This limitation can be resolved in future studies with the increase in the concentration of nanoparticles in the sealer. A reduction in the resistance to degradation was observed for this concentration, which can also may be adjusted in further analysis. The investigation of the long-term effect of these particles on the endodontic sealers showed that the maintenance of this effect over time may take place with the synthesized core-shell particles, being a useful source for local delivery of antibacterial compounds in endodontic sealers. In addition to this, the present study did not show an adverse cytotoxic effect with the incorporation of Ag@SiO<sub>2</sub> in the sealers, showing that the controlled composition and microstructure may be an alternative for the use of silver in endodontic applications.

Considering the aforementioned limitations, the challenge of this study is to be able to increase the antibacterial potential of the endodontic sealer, not causing a decrease in its physicochemical and biological properties. We suggest further studies for analyze concentrations with higher antibacterial potential.

## Conclusion

Based on the findings and within the limitations of this study the addition of 10 wt% Ag@SiO<sub>2</sub> reduced *E. faecalis* viability at immediate and longitudinal analysis while maintaining the physicochemical properties for developed sealers.

## References

- Abbasi, E. *et al.* (2016) 'Silver nanoparticles: Synthesis methods, bio-applications and properties', *Critical Reviews in Microbiology*, 42(2), pp. 173–180. Available at: <https://doi.org/10.3109/1040841X.2014.912200>.
- Ai, M. *et al.* (2017) 'Composite resin reinforced with silver nanoparticles-laden hydroxyapatite nanowires for dental application', *Dental Materials: Official Publication of the Academy of Dental Materials*, 33(1), pp. 12–22. Available at: <https://doi.org/10.1016/j.dental.2016.09.038>.
- Al-Hiyasat, A.S., Tayyar, M. and Darmani, H. (2010) 'Cytotoxicity evaluation of various resin based root canal sealers', *International Endodontic Journal*, 43(2), pp. 148–153. Available at: <https://doi.org/10.1111/j.1365-2591.2009.01669.x>.
- Ando, N. and Hoshino, E. (1990) 'Predominant obligate anaerobes invading the deep layers of root canal dentine', *International Endodontic Journal*, 23(1), pp. 20–27. Available at: <https://doi.org/10.1111/j.1365-2591.1990.tb00798.x>.



- Baras, B.H. *et al.* (2019) 'Novel root canal sealer with dimethylaminohexadecyl methacrylate, nano-silver and nano-calcium phosphate to kill bacteria inside root dentin and increase dentin hardness', *Dental Materials: Official Publication of the Academy of Dental Materials*, 35(10), pp. 1479–1489. Available at: <https://doi.org/10.1016/j.dental.2019.07.014>.
- Barros, J. *et al.* (2014) 'Antibacterial, physicochemical and mechanical properties of endodontic sealers containing quaternary ammonium polyethylenimine nanoparticles', *International Endodontic Journal*, 47(8), pp. 725–734. Available at: <https://doi.org/10.1111/iej.12207>.
- Belli, R. *et al.* (2014) 'Strengthening of dental adhesives via particle reinforcement', *Journal of the Mechanical Behavior of Biomedical Materials*, 37, pp. 100–108. Available at: <https://doi.org/10.1016/j.jmbbm.2014.05.007>.
- Benhadjala, W., Gravouelle, M. and Bord-Majek, I. (2015) 'Inorganic/organic nanocomposites: Reaching a high filler content without increasing viscosity using core-shell structured nanoparticles', *Appl. Phys. Lett.*, p. 5.
- Bodrumlu, E. and Semiz, M. (2006) 'Antibacterial Activity of a New Endodontic Sealer against *Enterococcus faecalis*', *Journal of the Canadian Dental Association*, 72(7), pp. 637–637c.
- Chakmakchi, M. *et al.* (2020) 'In vitro Assessment of Coronal Discoloration from Endodontic Sealers', *Al-Rafidain Dental Journal*, 20(2), pp. 177–182. Available at: <https://doi.org/10.33899/rden.2020.166457>.
- Chávez-Andrade, G.M. *et al.* (2017) 'Cytotoxicity, genotoxicity and antibacterial activity of poly(vinyl alcohol)-coated silver nanoparticles and farnesol as irrigating solutions', *Archives of Oral Biology*, 84, pp. 89–93. Available at: <https://doi.org/10.1016/j.archoralbio.2017.09.028>.
- Chen, L. *et al.* (2018) 'Inhibition of *Enterococcus faecalis* Growth and Biofilm Formation by Molecule Targeting Cyclic di-AMP Synthetase Activity', *Journal of Endodontics*, 44(9), pp. 1381–1388.e2. Available at: <https://doi.org/10.1016/j.joen.2018.05.008>.
- Cohen, M.S. *et al.* (2007) 'In vitro analysis of a nanocrystalline silver-coated surgical mesh', *Surgical Infections*, 8(3), pp. 397–403. Available at: <https://doi.org/10.1089/sur.2006.032>.
- Collares, F. *et al.* (2010) 'Ytterbium trifluoride as a radiopaque agent for dental cements', *International endodontic journal*, 43, pp. 792–7. Available at: <https://doi.org/10.1111/j.1365-2591.2010.01746.x>.
- Collares, F.M. *et al.* (2011) 'Influence of 2-Hydroxyethyl Methacrylate Concentration on Polymer Network of Adhesive Resin', *Journal of Adhesive Dentistry*, 13(2), pp. 125–129. Available at: <https://doi.org/10.3290/j.jad.a18781>.
- Corrêa, J.M. *et al.* (2015) 'Silver nanoparticles in dental biomaterials', *International Journal of Biomaterials*, 2015, p. 485275. Available at: <https://doi.org/10.1155/2015/485275>.
- Daming Wu *et al.* (2014) *Evaluation of the Antibacterial Efficacy of Silver Nanoparticles Against Enterococcus Faecalis Biofilm*, *Journal of endodontics*. J Endod. Available at: <https://doi.org/10.1016/j.joen.2013.08.022>.
- Degrazia, F.W. *et al.* (2016) 'Effect of silver nanoparticles on the physicochemical and antimicrobial properties of an orthodontic adhesive', *Journal of Applied Oral Science*, 24(4), pp. 404–410. Available at: <https://doi.org/10.1590/1678-775720160154>.

- Dhanalekshmi, K.I. *et al.* (2019) 'Preparation and characterization of core-shell type Ag@SiO<sub>2</sub> nanoparticles for photodynamic cancer therapy', *Photodiagnosis and Photodynamic Therapy*, 28, pp. 324–329. Available at: <https://doi.org/10.1016/j.pdpdt.2019.10.006>.
- Dhanalekshmi, K.I. and Meena, K.S. (2014) 'Comparison of antibacterial activities of Ag@TiO<sub>2</sub> and Ag@SiO<sub>2</sub> core-shell nanoparticles', *Spectrochimica Acta. Part A, Molecular and Biomolecular Spectroscopy*, 128, pp. 887–890. Available at: <https://doi.org/10.1016/j.saa.2014.02.063>.
- Drummond, J.L. (2008) 'Degradation, fatigue and failure of resin dental composite materials', *Journal of dental research*, 87(8), pp. 710–719.
- Ertem, E. *et al.* (2017) 'Core-Shell Silver Nanoparticles in Endodontic Disinfection Solutions Enable Long-Term Antimicrobial Effect on Oral Biofilms', *ACS applied materials & interfaces*, 9(40), pp. 34762–34772. Available at: <https://doi.org/10.1021/acsami.7b13929>.
- Feng, H.-P. *et al.* (2019) 'Core-shell nanomaterials: Applications in energy storage and conversion', *Advances in Colloid and Interface Science*, 267, pp. 26–46. Available at: <https://doi.org/10.1016/j.cis.2019.03.001>.
- Ferracane, J.L. (1985) 'Correlation between hardness and degree of conversion during the setting reaction of unfilled dental restorative resins', *Dental Materials*, 1(1), pp. 11–14. Available at: [https://doi.org/10.1016/S0109-5641\(85\)80058-0](https://doi.org/10.1016/S0109-5641(85)80058-0).
- Ferracane, J.L. (2006) 'Hygroscopic and hydrolytic effects in dental polymer networks', *Dental Materials: Official Publication of the Academy of Dental Materials*, 22(3), pp. 211–222. Available at: <https://doi.org/10.1016/j.dental.2005.05.005>.
- Ferracane, J.L., Berge, H.X. and Condon, J.R. (1998) 'In vitro aging of dental composites in water—Effect of degree of conversion, filler volume, and filler/matrix coupling', *Journal of Biomedical Materials Research*, 42(3), pp. 465–472. Available at: [https://doi.org/10.1002/\(SICI\)1097-4636\(19981205\)42:3<465::AID-JBM17>3.0.CO;2-F](https://doi.org/10.1002/(SICI)1097-4636(19981205)42:3<465::AID-JBM17>3.0.CO;2-F).
- Fukushima, H. *et al.* (1990) 'Localization and identification of root canal bacteria in clinically asymptomatic periapical pathosis', *Journal of Endodontics*, 16(11), pp. 534–538. Available at: [https://doi.org/10.1016/S0099-2399\(07\)80216-0](https://doi.org/10.1016/S0099-2399(07)80216-0).
- Guo, L. *et al.* (2019) 'Facile core-shell nanoparticles with controllable antibacterial activity assembled by chemical and biological molecules', *Biomaterials Science*, 7(12), pp. 5528–5534. Available at: <https://doi.org/10.1039/c9bm01367a>.
- Habib, E., Wang, R. and Zhu, X.X. (2018) 'Correlation of resin viscosity and monomer conversion to filler particle size in dental composites', *Dental Materials*, 34(10), pp. 1501–1508. Available at: <https://doi.org/10.1016/j.dental.2018.06.008>.
- Hao-peng Feng *et al.* (2019) 'Core-shell nanomaterials: Applications in energy storage and conversion', *Advances in Colloid and Interface Science*, 267, pp. 26–46. Available at: <https://doi.org/10.1016/j.cis.2019.03.001>.
- He, W. *et al.* (2015) 'Core-shell structured gel-nanocarriers for sustained drug release and enhanced antitumor effect', *International Journal of Pharmaceutics*, 484(1–2), pp. 163–171. Available at: <https://doi.org/10.1016/j.ijpharm.2015.02.053>.

Howard, B. *et al.* (2010) 'Relationships between conversion, temperature and optical properties during composite photopolymerization', *Acta Biomaterialia*, 6(6), pp. 2053–2059. Available at: <https://doi.org/10.1016/j.actbio.2009.11.006>.

International Organization for Standardization. Dentistry-Root Canal Sealing Materials. ISO 6876. London, UK: British Standards Institution (2012) 'ISO 6876:2012 - Dentistry - Root canal sealing materials'.

Jung, W.K. *et al.* (2008) 'Antibacterial activity and mechanism of action of the silver ion in Staphylococcus aureus and Escherichia coli', *Applied and Environmental Microbiology*, 74(7), pp. 2171–2178. Available at: <https://doi.org/10.1128/AEM.02001-07>.

Kapil Jhajharia *et al.* (2015) *Biofilm in endodontics: A review*. Available at: <https://go-gale.ez45.periodicos.capes.gov.br/ps/i.do?p=AONE&u=capes&id=GALE|A403254477&v=2.1&it=r> (Accessed: 16 May 2020).

Keiko Yamaki *et al.* (2012) *Rapid Quantification of Bacteria in Infected Root Canals Using Fluorescence Reagents and a Membrane Filter: A Pilot Study on Its Clinical Application to the Evaluation of the Outcomes of Endodontic Treatment*. Available at: <https://www.hindawi.com/journals/ijjd/2012/172935/> (Accessed: 22 May 2020).

Kirmanidou, Y. *et al.* (2019) 'Assessment of cytotoxicity and antibacterial effects of silver nanoparticle-doped titanium alloy surfaces', *Dental Materials: Official Publication of the Academy of Dental Materials*, 35(9), pp. e220–e233. Available at: <https://doi.org/10.1016/j.dental.2019.06.003>.

Kishen, A. *et al.* (2008) 'An investigation on the antibacterial and antibiofilm efficacy of cationic nanoparticulates for root canal disinfection', *Journal of Endodontics*, 34(12), pp. 1515–1520. Available at: <https://doi.org/10.1016/j.joen.2008.08.035>.

Klasen, H.J. (2000) 'Historical review of the use of silver in the treatment of burns. I. Early uses', *Burns: Journal of the International Society for Burn Injuries*, 26(2), pp. 117–130. Available at: [https://doi.org/10.1016/s0305-4179\(99\)00108-4](https://doi.org/10.1016/s0305-4179(99)00108-4).

Kris N. J. Stevens *et al.* (2009) 'The relationship between the antimicrobial effect of catheter coatings containing silver nanoparticles and the coagulation of contacting blood', *Biomaterials*, 30(22), pp. 3682–3690. Available at: <https://doi.org/10.1016/j.biomaterials.2009.03.054>.

Lea Assed Bezerra Silva *et al.* (2014) 'Sealapex Xpress and RealSeal XT Feature Tissue Compatibility In Vivo', *Journal of Endodontics*, 40(9), pp. 1424–1428. Available at: <https://doi.org/10.1016/j.joen.2014.01.040>.

Lee, B.-S. *et al.* (2011) 'A Novel Urethane Acrylate-based Root Canal Sealer with Improved Degree of Conversion, Cytotoxicity, Bond Strengths, Solubility, and Dimensional Stability', *Journal of Endodontics*, 37(2), pp. 246–249. Available at: <https://doi.org/10.1016/j.joen.2010.11.008>.

Leitune, V.C.B. *et al.* (2013) 'Niobium pentoxide as a novel filler for dental adhesive resin', *Journal of Dentistry*, 41(2), pp. 106–113. Available at: <https://doi.org/10.1016/j.jdent.2012.04.022>.

Lin, L.M. *et al.* (1991) 'Clinical, radiographic, and histologic study of endodontic treatment failures', *Oral Surgery, Oral Medicine, Oral Pathology*, 71(5), pp. 603–611. Available at: [https://doi.org/10.1016/0030-4220\(91\)90371-I](https://doi.org/10.1016/0030-4220(91)90371-I).

Liu, X. *et al.* (2017) 'One-pot preparation of nanoporous Ag-Cu@Ag core-shell alloy with enhanced oxidative stability and robust antibacterial activity', *Scientific Reports*, 7(1), p. 10249. Available at: <https://doi.org/10.1038/s41598-017-10630-5>.

Loyola-Rodríguez, J.P. *et al.* (2019) 'Antimicrobial activity of endodontic sealers and medications containing chitosan and silver nanoparticles against *Enterococcus faecalis*', *Journal of Applied Biomaterials & Functional Materials*, 17(3), p. 2280800019851771. Available at: <https://doi.org/10.1177/2280800019851771>.

Marin, S. *et al.* (2015) 'Applications and toxicity of silver nanoparticles: a recent review', *Current Topics in Medicinal Chemistry*, 15(16), pp. 1596–1604. Available at: <https://doi.org/10.2174/1568026615666150414142209>.

Michelsen, V.B. *et al.* (2008) 'Quantitative analysis of TEGDMA and HEMA eluted into saliva from two dental composites by use of GC/MS and tailor-made internal standards', *Dental Materials: Official Publication of the Academy of Dental Materials*, 24(6), pp. 724–731. Available at: <https://doi.org/10.1016/j.dental.2007.08.002>.

Nair, P.N.R. (2006) 'On the causes of persistent apical periodontitis: a review', *International Endodontic Journal*, 39(4), pp. 249–281. Available at: <https://doi.org/10.1111/j.1365-2591.2006.01099.x>.

Nathanson, M. *et al.* (2018) 'Atomic-Scale Structure and Stress Release Mechanism in Core-Shell Nanoparticles', *ACS nano*, 12(12), pp. 12296–12304. Available at: <https://doi.org/10.1021/acsnano.8b06118>.

Pearson, G.J. and Longman, C.M. (1989) 'Water sorption and solubility of resin-based materials following inadequate polymerization by a visible-light curing system', *Journal of Oral Rehabilitation*, 16(1), pp. 57–61. Available at: <https://doi.org/10.1111/j.1365-2842.1989.tb01317.x>.

Perez, R.A. and Kim, H.-W. (2015) 'Core-shell designed scaffolds for drug delivery and tissue engineering', *Acta Biomaterialia*, 21, pp. 2–19. Available at: <https://doi.org/10.1016/j.actbio.2015.03.013>.

Rajasekharreddy, P. and Rani, P.U. (2014) 'Biofabrication of Ag nanoparticles using *Sterculia foetida* L. seed extract and their toxic potential against mosquito vectors and HeLa cancer cells', *Materials Science & Engineering. C, Materials for Biological Applications*, 39, pp. 203–212. Available at: <https://doi.org/10.1016/j.msec.2014.03.003>.

Riaz Ahmed, K.B. *et al.* (2017) 'Silver nanoparticles: Significance of physicochemical properties and assay interference on the interpretation of in vitro cytotoxicity studies', *Toxicology in vitro: an international journal published in association with BIBRA*, 38, pp. 179–192. Available at: <https://doi.org/10.1016/j.tiv.2016.10.012>.

Rodrigues, M.C. *et al.* (2020) 'Biogenic synthesis and antimicrobial activity of silica-coated silver nanoparticles for esthetic dental applications', *Journal of Dentistry*, 96, p. 103327. Available at: <https://doi.org/10.1016/j.jdent.2020.103327>.

Roguska, A. *et al.* (2012) 'Evaluation of the Antibacterial Activity of Ag-Loaded TiO<sub>2</sub> Nanotubes', *European Journal of Inorganic Chemistry*, 2012(32), pp. 5199–5206. Available at: <https://doi.org/10.1002/ejic.201200508>.

- Rostirolla, F.V. *et al.* (2019) 'Calcium phosphates as fillers for methacrylate-based sealer', *Clinical Oral Investigations*, 23(12), pp. 4417–4423. Available at: <https://doi.org/10.1007/s00784-019-02898-w>.
- Sedgley, C.M., Lennan, S.L. and Appelbe, O.K. (2005) 'Survival of *Enterococcus faecalis* in root canals *ex vivo*', *International Endodontic Journal*, 38(10), pp. 735–742. Available at: <https://doi.org/10.1111/j.1365-2591.2005.01009.x>.
- Shrestha, A. and Kishen, A. (2016) 'Antibacterial Nanoparticles in Endodontics: A Review', *Journal of Endodontics*, 42(10), pp. 1417–1426. Available at: <https://doi.org/10.1016/j.joen.2016.05.021>.
- Shrivastava, S. *et al.* (2007) 'Characterization of enhanced antibacterial effects of novel silver nanoparticles', *Nanotechnology*, 18(22), p. 225103. Available at: <https://doi.org/10.1088/0957-4484/18/22/225103>.
- da Silva, E.M. *et al.* (2008) 'Relationship between the degree of conversion, solubility and salivary sorption of a hybrid and a nanofilled resin composite', *Journal of applied oral science: revista FOB*, 16(2), pp. 161–166. Available at: <https://doi.org/10.1590/s1678-77572008000200015>.
- Silver, S., Phung, L.T. and Silver, G. (2006) 'Silver as biocides in burn and wound dressings and bacterial resistance to silver compounds', *Journal of Industrial Microbiology & Biotechnology*, 33(7), pp. 627–634. Available at: <https://doi.org/10.1007/s10295-006-0139-7>.
- Singh, P., Kim, Y.J. and Yang, D.C. (2016) 'A strategic approach for rapid synthesis of gold and silver nanoparticles by *Panax ginseng* leaves', *Artificial Cells, Nanomedicine, and Biotechnology*, 44(8), pp. 1949–1957. Available at: <https://doi.org/10.3109/21691401.2015.1115410>.
- Siqueira, J.F. (2001) 'Aetiology of root canal treatment failure: why well-treated teeth can fail', *International Endodontic Journal*, 34(1), pp. 1–10. Available at: <https://doi.org/10.1046/j.1365-2591.2001.00396.x>.
- Siqueira Jr., J.F., Fraga, R.C. and Garcia, P.F. (1995) 'Evaluation of sealing ability, pH and flow rate of three calcium hydroxide-based sealers', *Endodontics & Dental Traumatology*, 11(5), pp. 225–228. Available at: <https://doi.org/10.1111/j.1600-9657.1995.tb00493.x>.
- Slutzky-Goldberg, I. *et al.* (2008) 'Antibacterial Properties of Four Endodontic Sealers', *Journal of Endodontics*, 34(6), pp. 735–738. Available at: <https://doi.org/10.1016/j.joen.2008.03.012>.
- Sofi, W. *et al.* (2012) 'Silver nanoparticles as an antibacterial agent for endodontic infections', *BMC Infectious Diseases*, 12(1), p. P60. Available at: <https://doi.org/10.1186/1471-2334-12-S1-P60>.
- Stansbury, J.W. and Dickens, S.H. (2001) 'Determination of double bond conversion in dental resins by near infrared spectroscopy', *Dental Materials: Official Publication of the Academy of Dental Materials*, 17(1), pp. 71–79. Available at: [https://doi.org/10.1016/s0109-5641\(00\)00062-2](https://doi.org/10.1016/s0109-5641(00)00062-2).
- Stöber, W., Fink, A. and Bohn, E. (1968) 'Controlled growth of monodisperse silica spheres in the micron size range', *Journal of Colloid and Interface Science*, 26(1), pp. 62–69. Available at: [https://doi.org/10.1016/0021-9797\(68\)90272-5](https://doi.org/10.1016/0021-9797(68)90272-5).

Sundqvist, G. *et al.* (1998) 'Microbiologic analysis of teeth with failed endodontic treatment and the outcome of conservative re-treatment', *Oral Surgery, Oral Medicine, Oral Pathology, Oral Radiology, and Endodontology*, 85(1), pp. 86–93. Available at: [https://doi.org/10.1016/S1079-2104\(98\)90404-8](https://doi.org/10.1016/S1079-2104(98)90404-8).

Takamiya, A.S. *et al.* (2016) 'In Vitro and In Vivo Toxicity Evaluation of Colloidal Silver Nanoparticles Used in Endodontic Treatments', *Journal of Endodontics*, 42(6), pp. 953–960. Available at: <https://doi.org/10.1016/j.joen.2016.03.014>.

Tan, P. *et al.* (2016) 'Core–Shell AgCl@SiO<sub>2</sub> Nanoparticles: Ag(I)-Based Antibacterial Materials with Enhanced Stability', *ACS Sustainable Chemistry & Engineering*, 4(6), pp. 3268–3275. Available at: <https://doi.org/10.1021/acssuschemeng.6b00309>.

Teixeira, A.B.V. *et al.* (2020) 'Cytotoxicity and release ions of endodontic sealers incorporated with a silver and vanadium base nanomaterial', *Odontology* [Preprint]. Available at: <https://doi.org/10.1007/s10266-020-00507-x>.

Videira-Quintela, D. *et al.* (2020) 'Silver, copper, and copper hydroxy salt decorated fumed silica hybrid composites as antibacterial agents', *Colloids and Surfaces B: Biointerfaces*, 195, p. 111216. Available at: <https://doi.org/10.1016/j.colsurfb.2020.111216>.

Yamanaka, M., Hara, K. and Kudo, J. (2005) 'Bactericidal actions of a silver ion solution on *Escherichia coli*, studied by energy-filtering transmission electron microscopy and proteomic analysis', *Applied and Environmental Microbiology*, 71(11), pp. 7589–7593. Available at: <https://doi.org/10.1128/AEM.71.11.7589-7593.2005>.

Yang, X.-L. *et al.* (2016) 'Core-Shell Chitosan Microcapsules for Programmed Sequential Drug Release', *ACS applied materials & interfaces*, 8(16), pp. 10524–10534. Available at: <https://doi.org/10.1021/acsaami.6b01277>.

Zhang, H. *et al.* (2009) 'Antibacterial Activity of Endodontic Sealers by Modified Direct Contact Test Against *Enterococcus faecalis*', *Journal of Endodontics*, 35(7), pp. 1051–1055. Available at: <https://doi.org/10.1016/j.joen.2009.04.022>.

Zhao, L. *et al.* (2011) 'Antibacterial nano-structured titania coating incorporated with silver nanoparticles', *Biomaterials*, 32(24), pp. 5706–5716. Available at: <https://doi.org/10.1016/j.biomaterials.2011.04.040>.

#### 4 CONSIDERAÇÕES FINAIS

Novas tecnologias e novas abordagens são utilizadas na área de materiais dentários como uma tentativa de reduzir a taxa de falhas dos tratamentos odontológicos realizados. A adição de agentes antibacterianos na composição dos cimentos endodônticos, por exemplo, pode ser utilizada como uma estratégia para diminuir os riscos de recontaminação do sistema de canais radiculares após o tratamento endodôntico. O grande desafio do desenvolvimento de materiais com ação antibacteriana é promover esta ação mantendo as propriedades físico-químicas, mecânicas e biológicas adequadas.

A prata é utilizada em diversas áreas como um agente antimicrobiano eficaz, porém sabe-se que os íons  $\text{Ag}^+$  possuem potencial citotóxico. As nanopartículas *core-shell*, por outro lado, vêm sendo estudadas e utilizadas como carreadores de íons, possibilitando que estes sejam liberados de maneira controlada, podendo promover uma maior biocompatibilidade ao material.

No presente estudo, as  $\text{Ag@SiO}_2$  foram sintetizadas adequadamente. As análises feitas mostraram a presença de prata no centro das nanopartículas *core-shell*. Além disso, também podemos identificar a presença de uma estrutura de casca esférica cinza escura bem definida, que pode ser atribuída à presença de sílica nas partículas. A adição de até 10% de  $\text{Ag@SiO}_2$  em peso não afetou as propriedades físico-químicas ou a sua biocompatibilidade. Além disso, o grupo com a adição de 10% mostrou redução na viabilidade de *E. faecalis*, e esta ação se manteve na análise longitudinal de 9 meses.

O presente estudo possui algumas limitações como o fato de que a redução na contagem de unidades formadoras de colônias foi inferior a 2 log. Apesar disso, o resultado representa uma atividade antibacteriana e continua sendo relevante, principalmente porque a atividade antibacteriana também foi encontrada na análise longitudinal de 9 meses, indicando que há uma liberação sustentada de prata pelo material. Também no grupo 10% uma maior taxa de amolecimento em solvente foi encontrada, sendo traduzida como uma maior degradação do material. Essa degradação se relaciona com uma diminuição das propriedades do cimento. Os grupos também não apresentaram a radiopacidade esperada e exigida pela ISO 6876. Em estudos futuros essas limitações poderiam ser solucionadas, utilizando compostos que tentem amenizar os efeitos da adição das  $\text{Ag@SiO}_2$ . Com os resultados obtidos podemos concluir que as  $\text{Ag@SiO}_2$  possuem potencial para promover ação antibacteriana aos materiais dentários.

## REFERÊNCIAS

- ABBASI, E. et al. Silver nanoparticles: Synthesis methods, bio-applications and properties. **Critical Reviews in Microbiology**, p. 1–8, 17 jun. 2014.
- ABDULLAH, M. et al. Susceptibilities of Two Enterococcus faecalis Phenotypes to Root Canal Medications. **Journal of Endodontics**, v. 31, n. 1, p. 30–36, 1 jan. 2005.
- ABDULWAHAB, M. A. et al. Persistence of bacteria and its role in endodontic treatment failure. **International Journal Of Community Medicine And Public Health**, v. 9, n. 1, p. 432–436, 27 dez. 2021.
- ALIMUNNISA, J.; RAVICHANDRAN, K.; MEENA, K. S. Synthesis and characterization of Ag@SiO<sub>2</sub> core-shell nanoparticles for antibacterial and environmental applications. **Journal of Molecular Liquids**, v. 231, p. 281–287, 1 abr. 2017.
- ALLAKER, R. P. The Use of Nanoparticles to Control Oral Biofilm Formation. **Journal of Dental Research**, v. 89, n. 11, p. 1175–1186, nov. 2010.
- ANTON, N.; BENOIT, J.-P.; SAULNIER, P. Design and production of nanoparticles formulated from nano-emulsion templates-a review. **Journal of Controlled Release: Official Journal of the Controlled Release Society**, v. 128, n. 3, p. 185–199, 24 jun. 2008.
- BARAS, B. H. et al. Novel root canal sealer with dimethylaminohexadecyl methacrylate, nano-silver and nano-calcium phosphate to kill bacteria inside root dentin and increase dentin hardness. **Dental Materials: Official Publication of the Academy of Dental Materials**, v. 35, n. 10, p. 1479–1489, 2019.
- CHEN, L. et al. Inhibition of Enterococcus faecalis Growth and Biofilm Formation by Molecule Targeting Cyclic di-AMP Synthetase Activity. **Journal of Endodontics**, v. 44, n. 9, p. 1381- 1388.e2, set. 2018.
- COHEN, M. S. et al. In vitro analysis of a nanocrystalline silver-coated surgical mesh. **Surgical Infections**, v. 8, n. 3, p. 397–403, jun. 2007.
- CORRÊA, J. M. et al. Silver nanoparticles in dental biomaterials. **International Journal of Biomaterials**, v. 2015, p. 485275, 2015.
- DE PAZ, L. C. Redefining the Persistent Infection in Root Canals: Possible Role of Biofilm Communities. **Journal of Endodontics**, v. 33, n. 6, p. 652–662, jun. 2007.
- DHANALEKSHMI, K. I.; MEENA, K. S. Comparison of antibacterial activities of Ag@TiO<sub>2</sub> and Ag@SiO<sub>2</sub> core-shell nanoparticles. **Spectrochimica Acta. Part A, Molecular and Biomolecular Spectroscopy**, v. 128, p. 887–890, 15 jul. 2014.
- ELEMAM, R. F.; PRETTY, I. Comparison of the success rate of endodontic treatment and implant treatment. **ISRN dentistry**, v. 2011, p. 640509, 2011.
- ERTEM, E. et al. Core-Shell Silver Nanoparticles in Endodontic Disinfection Solutions Enable Long-Term Antimicrobial Effect on Oral Biofilms. **ACS applied materials & interfaces**, v. 9, n. 40, p. 34762–34772, 11 out. 2017.



- HE, W. et al. Core-shell structured gel-nanocarriers for sustained drug release and enhanced antitumor effect. **International Journal of Pharmaceutics**, v. 484, n. 1–2, p. 163–171, 30 abr. 2015.
- ISAACS, M. A. et al. Tunable Ag@SiO<sub>2</sub> core-shell nanocomposites for broad spectrum antibacterial applications. **RSC Advances**, v. 7, n. 38, p. 23342–23347, 27 abr. 2017.
- JEEVANANDAM, J. et al. Review on nanoparticles and nanostructured materials: history, sources, toxicity and regulations. **Beilstein Journal of Nanotechnology**, v. 9, p. 1050–1074, 3 abr. 2018.
- JUNG, W. K. et al. Antibacterial activity and mechanism of action of the silver ion in *Staphylococcus aureus* and *Escherichia coli*. **Applied and Environmental Microbiology**, v. 74, n. 7, p. 2171–2178, abr. 2008.
- KASHANI, S. Y. et al. Microfluidics for core-shell drug carrier particles – a review. **RSC Advances**, v. 11, n. 1, p. 229–249, 21 dez. 2020.
- KIM, J. S. et al. Antimicrobial effects of silver nanoparticles. **Nanomedicine: Nanotechnology, Biology and Medicine**, v. 3, n. 1, p. 95–101, 1 mar. 2007.
- KIRMANIDOU, Y. et al. Assessment of cytotoxicity and antibacterial effects of silver nanoparticle-doped titanium alloy surfaces. **Dental Materials**, v. 35, n. 9, p. e220–e233, 1 set. 2019.
- KLASEN, H. J. Historical review of the use of silver in the treatment of burns. I. Early uses. **Burns: Journal of the International Society for Burn Injuries**, v. 26, n. 2, p. 117–130, mar. 2000.
- KRIS N. J. STEVENS et al. The relationship between the antimicrobial effect of catheter coatings containing silver nanoparticles and the coagulation of contacting blood. **Biomaterials**, v. 30, n. 22, p. 3682–3690, 1 ago. 2009.
- LIU, X. et al. One-pot preparation of nanoporous Ag-Cu@Ag core-shell alloy with enhanced oxidative stability and robust antibacterial activity. **Scientific Reports**, v. 7, 31 ago. 2017.
- LOYOLA-RODRÍGUEZ, J. P. et al. Antimicrobial activity of endodontic sealers and medications containing chitosan and silver nanoparticles against *Enterococcus faecalis*. **Journal of Applied Biomaterials & Functional Materials**, v. 17, n. 3, p. 2280800019851771, set. 2019.
- LU, Z. et al. Size-dependent antibacterial activities of silver nanoparticles against oral anaerobic pathogenic bacteria. **Journal of Materials Science: Materials in Medicine**, v. 24, n. 6, p. 1465–1471, jun. 2013.
- MONTEIRO, D. R. et al. The growing importance of materials that prevent microbial adhesion: antimicrobial effect of medical devices containing silver. **International Journal of Antimicrobial Agents**, v. 34, n. 2, p. 103–110, 1 ago. 2009.
- MORONES, J. R. et al. The bactericidal effect of silver nanoparticles. **Nanotechnology**, v. 16, n. 10, p. 2346, 26 ago. 2005.

NAIR, P. N. R. On the causes of persistent apical periodontitis: a review. **International Endodontic Journal**, v. 39, n. 4, p. 249–281, abr. 2006.

NATHANSON, M. et al. Atomic-Scale Structure and Stress Release Mechanism in Core–Shell Nanoparticles. **ACS Nano**, v. 12, n. 12, p. 12296–12304, 26 dez. 2018.

PEREZ, R. A.; KIM, H.-W. Core-shell designed scaffolds for drug delivery and tissue engineering. **Acta Biomaterialia**, v. 21, p. 2–19, jul. 2015.

RAI, M. K. et al. Silver nanoparticles: the powerful nanoweapon against multidrug-resistant bacteria. **Journal of Applied Microbiology**, v. 112, n. 5, p. 841–852, 2012.

RIAZ AHMED, K. B. et al. Silver nanoparticles: Significance of physicochemical properties and assay interference on the interpretation of in vitro cytotoxicity studies. **Toxicology in Vitro**, v. 38, p. 179–192, 1 fev. 2017.

RICUCCI, D. et al. Histologic investigation of root canal-treated teeth with apical periodontitis: a retrospective study from twenty-four patients. **Journal of Endodontics**, v. 35, n. 4, p. 493–502, abr. 2009.

RODRIGUES, C. T. et al. Antibacterial properties of silver nanoparticles as a root canal irrigant against *Enterococcus faecalis* biofilm and infected dentinal tubules. **International Endodontic Journal**, v. 51, n. 8, p. 901–911, ago. 2018.

SEDGLEY, C. M.; LENNAN, S. L.; APPELBE, O. K. Survival of *Enterococcus faecalis* in root canals ex vivo. **International Endodontic Journal**, v. 38, n. 10, p. 735–742, out. 2005.

SHRESTHA, A.; KISHEN, A. Antibacterial Nanoparticles in Endodontics: A Review. **Journal of Endodontics**, v. 42, n. 10, p. 1417–1426, out. 2016.

SHRIVASTAVA, S. et al. Characterization of enhanced antibacterial effects of novel silver nanoparticles. **Nanotechnology**, v. 18, n. 22, p. 225103, maio 2007.

SILVER, S.; PHUNG, L. T.; SILVER, G. Silver as biocides in burn and wound dressings and bacterial resistance to silver compounds. **Journal of Industrial Microbiology & Biotechnology**, v. 33, n. 7, p. 627–634, jul. 2006.

SIQUEIRA, J. F. Aetiology of root canal treatment failure: why well-treated teeth can fail. **International Endodontic Journal**, v. 34, n. 1, p. 1–10, 2001.

SUNDQVIST, G. et al. Microbiologic analysis of teeth with failed endodontic treatment and the outcome of conservative re-treatment. **Oral Surgery, Oral Medicine, Oral Pathology, Oral Radiology, and Endodontology**, v. 85, n. 1, p. 86–93, 1 jan. 1998.

TABASSUM, S.; KHAN, F. R. Failure of endodontic treatment: The usual suspects. **European Journal of Dentistry**, v. 10, n. 1, p. 144–147, mar. 2016.

TAKAMIYA, A. S. et al. In Vitro and In Vivo Toxicity Evaluation of Colloidal Silver Nanoparticles Used in Endodontic Treatments. **Journal of Endodontics**, v. 42, n. 6, p. 953–960, jun. 2016.

TAN, P. et al. Core–Shell AgCl@SiO<sub>2</sub> Nanoparticles: Ag(I)-Based Antibacterial Materials with Enhanced Stability. **ACS Sustainable Chemistry & Engineering**, v. 4, n. 6, p. 3268–3275, 6 jun. 2016.

WILSON, C. E. et al. Clonal diversity in biofilm formation by *Enterococcus faecalis* in response to environmental stress associated with endodontic irrigants and medicaments. **International Endodontic Journal**, v. 48, n. 3, p. 210–219, mar. 2015.

YAMANAKA, M.; HARA, K.; KUDO, J. Bactericidal actions of a silver ion solution on *Escherichia coli*, studied by energy-filtering transmission electron microscopy and proteomic analysis. **Applied and Environmental Microbiology**, v. 71, n. 11, p. 7589–7593, nov. 2005.

YANG, X.-L. et al. Core–Shell Chitosan Microcapsules for Programmed Sequential Drug Release. **ACS Applied Materials & Interfaces**, v. 8, n. 16, p. 10524–10534, 27 abr. 2016.